Multi-Modal Interactive Agent Layer for Few-Shot Universal Cross-Domain Retrieval and Beyond

Kaixiang Chen[1,2], **Pengfei Fang**[1,2*] , **Hui Xue**[1,2*]
[1]School of Computer Science and Engineering, Southeast University
[2]Key Laboratory of New Generation Artificial Intelligence Technology
and Its Interdisciplinary Applications (Southeast University), Ministry of Education, China
{kxchen, fangpengfei, hxue}@seu.edu.cn

Abstract

This paper firstly addresses the challenge of few-shot universal cross-domain retrieval (FS-UCDR), enabling machines trained with limited data to generalize to novel retrieval scenarios, with queries from entirely unknown domains and categories. To achieve this, we first formally define the FS-UCDR task and propose the **M**ulti-Mod**a**l **I**nteractive Agent **L**ayer (MAIL), which enhances the cross-modal interaction in vision-language models (VLMs) by aligning the parameter updates of target layer pairs across modalities. Specifically, MAIL freezes the selected target layer pair and introduces a trainable agent layer pair to approximate localized parameter updates. A bridge function is then introduced to couple the agent layer pair, enabling gradient communication across modalities to facilitate update alignment. The proposed MAIL offers four key advantages: **1)** its cross-modal interaction mechanism improves knowledge acquisition from limited data, making it highly effective in low-data scenarios; **2)** during inference, MAIL integrates seamlessly into the VLM via reparameterization, preserving inference complexity; **3)** extensive experiments validate the superiority of MAIL, which achieves substantial performance gains over data-efficient UCDR methods while requiring significantly fewer training samples; **4)** beyond UCDR, MAIL also performs competitively on few-shot classification tasks, underscoring its strong generalization ability. **Code**.

1 Introduction

The objective of universal cross-domain retrieval (UCDR) [37, 3] is to retrieve images from the real world (*Real* domain) using queries originating from unseen domains and classes. To achieve robust performance in these generalized retrieval scenarios, UCDR methods typically require extensive, diverse, and well-annotated datasets from multiple domains to learn domain-agnostic feature embeddings [37, 43, 13]. However, labeling data across multiple domains in real-world scenarios is often prohibitively expensive. More critically, in the UCDR task, the substantial domain gap between training and testing domains implies that excessive reliance on source domain data may lead to overfitting and poor generalization to unseen domains. Given

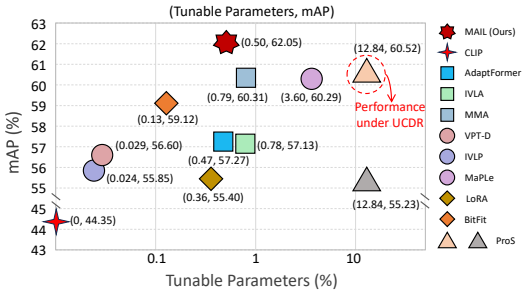

Figure 1: Comparison of MAIL with various methods on DomainNet [38] dataset under FS-UCDR (2-shot). The symbol □ indicates adapter-based methods, ◯ represents prompt-based methods, ◊ denotes partially fine-tuned methods, and △ denotes ProS [13], the SOTA method for UCDR.

*Co-corresponding authors

39th Conference on Neural Information Processing Systems (NeurIPS 2025).

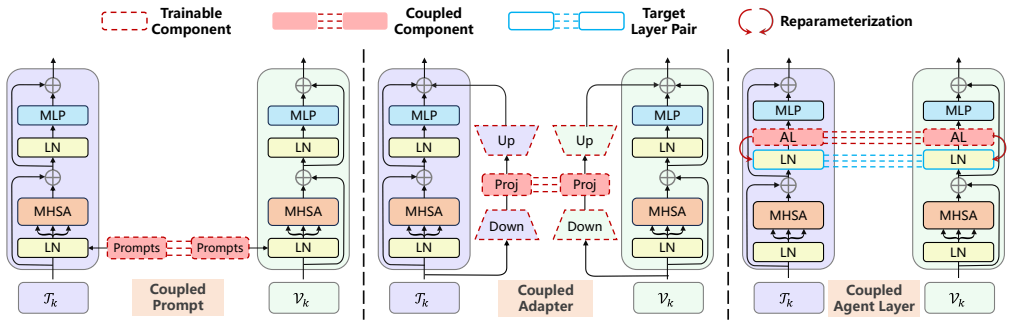

(a) MaPLe (b) MMA (c) Ours

Figure 2: Modality-coupled methods in fine-tuning VLMs: (a) MaPLe achieves multi-modal alignment by establishing interconnections between the prompts. (b) MMA designs a unified feature-projection layer within the adapter that is shared by both modalities. (c) In contrast, MAIL achieves multi-modal alignment while preserving inference efficiency by introducing linked trainable agent layers (AL) that align parameter updates without altering the original model structure.

that recent CLIP-based methods [39, 24, 49] have demonstrated strong performance in few-shot classification, indicating the potential to generalize well with limited supervision, this raises a natural question: *Is it possible to train a model using only a few samples from each domain to achieve performance comparable to, or even surpass, existing data-efficient UCDR methods?*

In response, this paper formally defines the problem of few-shot UCDR (FS-UCDR), which aims to train a retrieval model using minimal samples per class from each source domain. To address this challenge, we explore parameter-efficient fine-tuning (PEFT) for pretrained vision-language models (VLMs) like CLIP [39], whose remarkable "zero-shot" generalization capabilities position them as promising tools for the FS-UCDR problem. We first empirically conduct a comprehensive empirical study on fine-tuning CLIP under the FS-UCDR setting, covering **four** categories of methods: **three** types of PEFT methods—❶ *adapter-based methods* [6, 49], ❷ *prompt-based methods* [23, 24], and ❸ *partially fine-tuned methods* (either through direct tuning such as BitFit [52] or indirect tuning such as LoRA [22])—as well as ❹ the previous state-of-the-art UCDR method, ProS [13]. The results are shown in **Fig. 1**, where we observe that modality-coupled methods (MCMs) (e.g., MaPLe [24] and MMA [49]; see **Fig. 2-a** and **Fig. 2-b**) consistently outperform their modality-independent counterparts, i.e., independent vision-language prompt / adapter (IVLP / IVLA). Since the objective of vision–language training is to achieve effective alignment between modalities, the explicit cross-modal interactions inherent in MCMs strengthen this alignment and facilitate knowledge transfer from source domains, which is particularly valuable in low-data scenarios. Furthermore, cross-modal interaction can be interpreted as a form of regularization: such coupling ensures that updates in one modality are propagated to the other, thereby promoting more coherent and consistent representations.

Building upon the three explored types of PEFT methods, the first two—adapter-based and prompt-based methods—both include modality-coupled variants. However, modality coupling in the third type of PEFT methods has never been explored. This is primarily due to the non-trivial nature of such an endeavor. For instance, establishing cross-modal bias interactions in BitFit [52] or introducing modality coupling into the low-rank matrices of LoRA [22] poses significant challenges in both design and implementation. Given the unique advantage of the third type of PEFT methods—introducing no additional inference cost—designing a MCM for this category remains an important and yet underexplored problem. **To fill this gap**, this paper propose the **M**ulti-Mod**a**l **I**nteractive Agent **L**ayer (MAIL), which, to the best of our knowledge, is the **first** CLIP-based modality-coupled method explicitly aimed at enhancing the alignment of updates of the internal parameters between image and text modalities within the backbone, as illustrated in **Fig. 2-c**.

Specifically, to facilitate alignment updates between a specific pair of layers, MAIL designates these as the **target layer** pair while keeping their original parameters frozen. For each target layer, we introduce a lightweight **agent layer** that approximates the localized parameter updates through training. Each agent layer consists of a scaling and a shifting component [31], which together capture the fine-grained adjustments of the corresponding target layer. To encourage cross-modal interaction, we further incorporate a bridge function that couples the agent layers, enabling gradient flow between modalities during tuning and thereby strengthening alignment. At inference, the agent

layers are seamlessly reparameterized into their corresponding frozen layers, ensuring that the overall complexity of CLIP remains unchanged.

Compared to MaPLe and MMA, MAIL achieves superior performance with higher parameter efficiency in FS-UCDR and even surpasses ProS using only $1/140$ of the training data, as shown in **Fig. 1**. To summarize, our main contributions are outlined as follows: ❶ We formally define the problem of FS-UCDR and explore the potential of leveraging the pretrained vision-language model (VLM), specifically CLIP, to effectively address this challenge. ❷ We experimentally find that the modality-coupled method works effectively under FS-UCDR due to the explicit cross-modal interaction. ❸ We introduce MAIL, a novel MCM crafted to optimize the alignment of partially parameter updates across image and text modalities. ❹ Extensive experiments on *three* FS-UCDR benchmarks and *eleven* few-shot classification datasets demonstrate that MAIL achieves state-of-the-art performance while maintaining superior parameter efficiency and CLIP's inference efficiency.

2 Related Work

Universal Cross-Domain Retrieval. Cross-domain retrieval (CDR) [26, 16] addresses the inherent limitations of uni-domain retrieval (UDR) [5, 4, 42, 47] by enabling retrieval across diverse domains. However, it typically assumes that the testing phase involves known domains and semantic classes. This assumption restricts its applicability in real-world scenarios, where models often encounter entirely new domains and classes. Therefore, universal cross-domain retrieval (UCDR) [37, 43] has emerged as a promising direction, which leverages queries from unseen domains and unseen classes to retrieve semantically similar examples from the *Real* domain. However, this setup demands substantial data collection from diverse domains, which is both costly and time-intensive. To address these challenges, we propose a more practical and significantly more challenging variant: few-shot universal cross-domain retrieval (FS-UCDR), where only a limited number of samples per class are available for training, aiming to reduce data requirements while preserve retrieval effectiveness.

Parameter Efficient Fine-Tuning. With the rapid advancement of datasets, model architectures, and training algorithms [51, 7], foundation models like BERT [10], ViT [11], and CLIP [39] have revolutionized deep learning. However, their increasing size presents challenges for fine-tuning due to high memory and computational demands. To address these issues, parameter-efficient fine-tuning (PEFT) methods have been proposed, which can be broadly categorized into three types: ❶*Prompt-based methods.* These methods introduce additional learnable tokens during fine-tuning, while keeping all other parameters fixed. These tokens can be integrated into the vision model [23], the language model [57], or both [24], depending on the specific task requirements. ❷ *Adapter-based methods*. These methods incorporates lightweight adapter modules that are updated during fine-tuning, leaving the original model parameters unchanged. Adapters can take various forms, such as bottleneck structures [21, 6], simple residual layers [15], or memory banks [55, 54], and can be implemented either sequentially [21] or in parallel [6] with the original model. ❸ *Partially fine-tuned methods*. Some of these methods ***directly*** update a limited (target) subset of pretrained parameters, such as specific layers [1, 28] or biases [52], thereby minimizing overhead. Additionally, methods such as LoRA [22] and VeRA [27] ***indirectly*** approximate the partial updates by introducing new trainable parameters, which are merged back via re-parameterization to preserve inference efficiency.

3 Preliminary

3.1 Problem Setting

UCDR. In universal cross domain retrieval (UCDR), the training setup includes $N_S \geq 2$ source domains, collectively represented as $\mathbb{D}_S = \{\mathcal{D}_S^j\}_{j=1}^{N_S}$. Each domain is defined as $\mathcal{D}_S^j = \{(x_i^j, y_i^j)\}_{i=1}^{P_j}$, where x_i^j denotes the i-th image out of a total of P_j images in the j-th source domain, and y_i^j represents its class label from a **shared** label space $\mathcal{Y}_S$. Additionally, the *Real* domain $\mathcal{D}_R$, consists of real-word images, serves a dual purpose by contributing to both training and testing. Within $\mathcal{D}_R$, there are two distinct subdomains: $\mathcal{D}_R^+$ and $\mathcal{D}_R^-$. $\mathcal{D}_R^+$ is a subset belongs to $\mathbb{D}_S$, i.e., $\mathcal{D}_R^+ \in \mathbb{D}_S$. $\mathcal{D}_R^-$ serves as the **gallery set** during testing. In the test phase, a query set $\mathcal{D}_Q = \{(x_i^q, y_i^q)\}_{i=1}^{P_q}$ is also provided, containing P_q samples drawn from an unseen domain and unseen classes. By default, the classes in $\mathcal{D}_R^-$ are identical to those in $\mathcal{D}_Q$, and we denote this scenario as $\mathrm{UnseenGallery}$. However, in a realistic scenario, $\mathcal{D}_R^-$ may include additional classes, such as those from the training phase, which is refereed to as $\mathrm{MixedGallery}$.

U^{D}CDR and U^{C}CDR. Universal domain cross-domain retrieval (U^{D}CDR) and universal class cross-domain retrieval (U^{C}CDR) are two specialized variations of UCDR. In U^{D}CDR, the query class is encountered during training, while in U^{C}CDR, the query domain has been seen.

Few-Shot Setup. The aforementioned setups demand substantial data collection across diverse domains, which is costly and time-intensive. To this end, we propose a more practical few-shot setup. While the shared label space consists of C classes, we limit it to only k (a small number) shots per class for each domain, resulting in a total of $|\mathbb{D}_S| = N_S \times k \times C$ training samples.

3.2 Revisiting CLIP

CLIP [39] is a pretrained vision-language model (VLM) consisting of two encoders: a text encoder, denoted by $\mathcal{T}(\cdot)$, and an image encoder (ViT [11] as default), denoted by $\mathcal{V}(\cdot)$. Both encoders comprise L transformer [45] blocks, represented as $\{\mathcal{T}_i\}_{i=1}^{L}$ and $\{\mathcal{V}_i\}_{i=1}^{L}$, respectively. For classification inference with C classes, CLIP inserts all class names into a pre-defined text template, e.g., "`a photo of a <category>`", generating C inputs $\{t_i\}_{i=1}^{C}$ for the text encoder $\mathcal{T}(\cdot)$. For a certain input t_y, its output $\mathcal{T}(t_y)$ is:

$$\begin{aligned} \mathcal{W}_0 &= \text{TextEmbed}(t_y) \\ \mathcal{W}_i &= \mathcal{T}_i(\mathcal{W}_{i-1}), \quad i = 1, 2, ..., L \\ \mathcal{T}(t_y) &= \text{TextProj} \circ \text{LN}(w_L^{N_t}), \end{aligned} \tag{1}$$

where $\mathcal{W}_0 = [w_0^0, w_0^1, ..., w_0^{N_t}]^\top \in \mathbb{R}^{N_t \times d_t}$ is the word embedding, with N_t and d_t indicate text embedding length and dimension, $\circ$ represents the composition of functions. TextProj is a linear layer ($d_t \rightarrow d_t$). Similarly, for the image I, its representation $\mathcal{V}(I)$ is calculated as:

$$\begin{aligned} \mathcal{P}_0 &= \text{PatchEmbed}(I) \\ [c_i, \mathcal{P}_i] &= \mathcal{V}_i([c_{i-1}, \mathcal{P}_{i-1}]), \quad i = 1, 2, ..., L \\ \mathcal{V}(I) &= \text{ImageProj} \circ \text{LN}(c_L), \end{aligned} \tag{2}$$

where $\mathcal{P}_0 \in \mathbb{R}^{N_v \times d_v}$ is the image embedding, with N_v and d_v indicate embedding length and dimension, and $c_0 \in \mathbb{R}^{d_v}$ is the initial CLS Token. ImageProj is also a linear layer ($d_v \rightarrow d_t$). With $\mathcal{V}(I)$ available, the text features of the text templates with class labels are matched using the formula $p(y|I) = \frac{\exp(sim(\mathcal{T}(t_y), \mathcal{V}(I)))}{\sum_{i=1}^{C} \exp(sim(\mathcal{T}(t_i), \mathcal{V}(I)))}$, where $y \in \{1, 2, ..., C\}$, and $sim(.,.)$ refers to cosine similarity.

4 Multi-Modal Interactive Agent Layer

Modality-coupled methods (MCMs), such as MaPLe [24] and MMA [49], improve cross-modal alignment by enhancing synergy between encoders during training, thereby boosting retrieval performance under FS-UCDR. However, these benefits come with increased inference complexity. In contrast, the third type of PEFT methods—partially fine-tuned approaches—offers a key advantage: they introduce no additional inference overhead. Despite this, modality coupling has not been explored in this category. To bridge this gap, we propose the **M**ulti-Mod**a**l **I**nteractive Agent **L**ayer (MAIL), a lightweight MCM that aligns parameter updates across modalities while preserving the inference efficiency. As illustrated in **Fig. 3**, MAIL incorporates agent layers to capture localized parameter updates, while the bridge functions further refine and align these updates across encoders.

4.1 Agent Layer

The agent layer (AL) is designed to approximately capture the updates of specific operations within the encoders. It consists of **a scaling vector** a, initialized as an **all-one** vector, and **a shifting vector** b, initialized as an **all-zero** vector [31]. The agent layer can be appended after various positions:

$$\text{AL} \circ \text{OP}(x) = \text{OP}(x) \cdot \Lambda(a) + b, \tag{3}$$

where OP is a specific operation or a layer, $\Lambda(a)$ represents the diagonal matrix with the vector a as its diagonal elements, $\cdot$ denotes the matrix multiplication. In a transformer block, the agent layer can be positioned after the LayerNorm (LN) layer (***Position-1***) to capture updates related to the parameters of LN. Similarly, it can be placed after the multi-head self-attention (MHSA) layer (***Position-2***) to monitor updates to the output weight matrix W^O, or after the MLP layer (***Position-3***) to track changes in the second linear layer, W_{mlp}^2. Beyond the confines of transformer blocks, the agent layer can also be appended after the final LN layer (***Position-4***) and the last projection layer

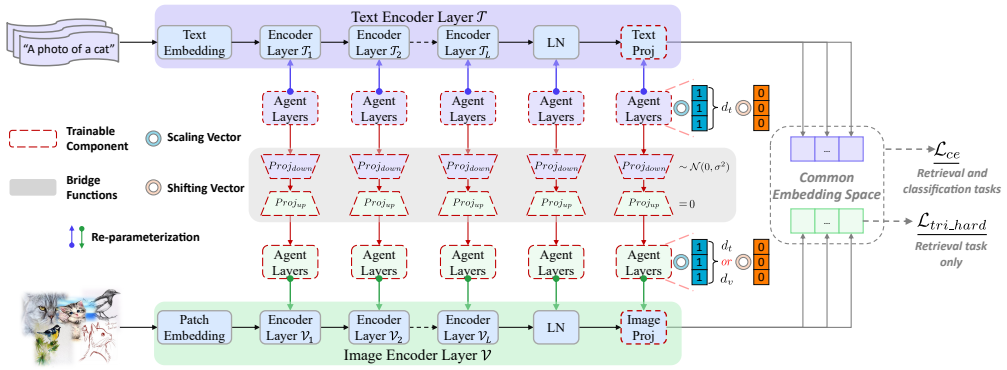

Figure 3: The proposed Multi-Modal Interactive Agent Layer (MAIL) for the transformer-based CLIP models. During training, we only fine-tune the agent layers, which are inserted into both encoders. The image agent layers interact with the text agent layers through a trainable bottleneck-based bridge function, fostering mutual synergy between the two modalities.

W_{proj} (***Position-5***), effectively capturing the relevant updates. One can refer to **Appendix G.4** for a clearer visual illustration. In summary, the agent layer is specifically designed to track updates for **five positions** from two types of layers: the LN layer and the linear layer. For illustrative purposes, we will focus on the text encoder (i.e., $a, b \in \mathbb{R}^{d_t}$) to demonstrate how updates occur in the LN and linear layers.

LN Layer: The LN operation is formulated as:

$$\mathrm{LN}(x) = \frac{x-\mu}{\sigma} \odot \gamma + \beta, \tag{4}$$

where $x \in \mathbb{R}^{N_t \times d_t}$ denotes the input to the LN layer, $\mu, \sigma \in \mathbb{R}^{N_t}$, $\gamma, \beta \in \mathbb{R}^{d_t}$. The agent layer, appended after the LN layer, can be formulated as:

$$\mathrm{AL} \circ \mathrm{LN}(x) = \frac{x-\mu}{\sigma} \odot \underbrace{\gamma \odot \underline{a}}_{\underline{\gamma}} + \underbrace{\beta \odot \underline{a} + \underline{b}}_{\underline{\beta}}, \tag{5}$$

where underline indicates the trainable component, and $\odot$ represents the Hadamard product. As shown in **Eq.** (5), the update of the agent layer can approximately correspond to the updates of γ and β in the LN layer.

Linear Layer: The linear layer is formulated as:

$$\mathrm{LiL}(x) = x \cdot W^\top + bias, \tag{6}$$

where $x \in \mathbb{R}^{N_t \times d_a}$ represents the input, with d_a can either equal to d_t or the intermediate dimension of the MLP layer within the transformer block. $W \in \mathbb{R}^{d_t \times d_a}$ denotes the weight matrix, and $bias \in \mathbb{R}^{d_t}$ represents the bias. The agent layer, appended after the linear layer, is expressed as:

$$\mathrm{AL} \circ \mathrm{LiL}(x) = x \cdot \underbrace{(\Lambda(\underline{a}) \cdot W)^\top}_{\underline{W}} + \underbrace{bias \odot \underline{a} + \underline{b}}_{\underline{bias}}. \tag{7}$$

Due to the left multiplication by $\Lambda(a)$ applied to W, the updates of W are row-wise.

During inference, based on **Eq.** (5) and **Eq.** (7), the agent layers can be seamlessly integrated into the original foundation model, **eliminating additional inference latency.**

4.2 Agent Layer Coupling

We define the text agent layer as $\mathrm{AL}_{\text{text}} = \{a_t, b_t \in \mathbb{R}^{d_t}\}$, and the image agent layer at the same location in the image encoder as $\mathrm{AL}_{\text{image}} = \{a_v, b_v \in \mathbb{R}^{d_v}\}$ or $\mathrm{AL}_{\text{image}} = \{a_v, b_v \in \mathbb{R}^{d_t}\}$ (when the agent layer is appended after the final projection layer). These agent layers can be trained independently, and we term such a design as *independent vision-language updating* (IVLU). To

Table 1: FS-UCDR (2-shot) evaluation results (%) on DomainNet. * denotes the results are obtained using the full training data, i.e., the UCDR results. The best performance under FS-UCDR is marked as **bold** and the second best performance is marked as underline, while scores from our method are highlighted with a light purple background.

Methods	*Sketch*				*Quickdraw*				*Painting*			
	UnseenGallery		**MixedGallery**		**UnseenGallery**		**MixedGallery**		**UnseenGallery**		**MixedGallery**	
	mAP_{200}	$Prec_{200}$	mAP_{200}	$Prec_{200}$	mAP_{200}	$Prec_{200}$	mAP_{200}	$Prec_{200}$	mAP_{200}	$Prec_{200}$	mAP_{200}	$Prec_{200}$
ProS* [CVPR'24]	64.67	60.01	58.43	54.63	28.42	25.44	23.18	21.27	75.16	69.55	71.20	66.12
CLIP [ICML'21]	42.20	35.28	36.62	29.79	7.44	5.61	6.00	3.17	61.68	55.07	56.53	50.14
BitFit [ACL'22]	62.68	57.71	55.84	51.52	24.88	21.99	19.22	16.93	73.40	67.39	68.46	62.93
LoRA [ICLR'22]	54.85	49.23	48.71	43.33	22.16	18.10	17.73	14.21	71.46	65.10	66.81	60.81
VPT-D [ECCV'22]	57.47	52.58	50.34	45.92	24.26	21.68	18.45	16.77	72.05	65.88	67.25	61.42
AFormer [NeurIPS'22]	59.64	53.73	52.91	47.77	23.11	19.86	18.11	15.71	71.08	64.59	66.14	60.17
IVLP [CVPR'23]	56.25	51.48	49.37	45.06	21.07	18.97	15.67	14.13	71.47	65.51	66.40	60.86
IVLA [CVPR'24]	60.01	54.16	53.27	48.19	23.96	20.72	18.74	16.38	71.02	64.60	66.10	60.18
MaPLe [CVPR'23]	62.50	57.49	55.69	51.67	27.57	24.93	21.58	19.75	75.02	69.41	70.61	65.38
MMA [CVPR'24]	63.86	58.84	56.74	52.33	27.37	24.28	21.84	19.56	74.08	68.36	69.24	63.92
MAIL [Ours]	**65.76**	**61.57**	**59.05**	**55.25**	**29.41**	**26.95**	**22.83**	**21.26**	**76.05**	**70.85**	**71.12**	**66.44**

Methods	*Infograph*				*Clipart*				*Average*			
	UnseenGallery		**MixedGallery**		**UnseenGallery**		**MixedGallery**		**UnseenGallery**		**MixedGallery**	
	mAP_{200}	$Prec_{200}$	mAP_{200}	$Prec_{200}$	mAP_{200}	$Prec_{200}$	mAP_{200}	$Prec_{200}$	mAP_{200}	$Prec_{200}$	mAP_{200}	$Prec_{200}$
ProS* [CVPR'24]	57.98	54.42	52.19	49.56	76.48	71.86	72.28	68.15	60.52	56.26	55.46	51.95
CLIP [ICML'21]	50.08	44.74	43.75	38.91	60.37	51.30	56.08	46.91	44.35	38.40	39.80	33.78
BitFit [ACL'22]	58.84	55.14	52.32	48.86	75.81	70.27	71.04	65.85	59.12	54.50	53.38	49.22
LoRA [ICLR'22]	58.01	53.84	51.86	48.20	70.52	64.11	66.00	59.63	55.40	50.08	50.22	45.24
VPT-D [ECCV'22]	56.28	52.18	49.61	45.92	72.96	67.82	68.02	63.04	56.60	52.20	50.73	46.61
AFormer [NeurIPS'22]	59.55	55.00	53.17	49.27	73.19	66.28	68.66	62.1	57.27	51.89	51.79	47.00
IVLP [CVPR'23]	58.20	54.07	51.60	47.89	72.28	66.98	67.64	62.47	55.85	51.42	50.13	46.08
IVLA [CVPR'24]	57.39	53.36	50.86	47.22	73.31	66.40	68.75	62.21	57.13	51.84	51.54	46.68
MaPLe [CVPR'23]	59.45	56.14	53.05	49.95	76.92	72.28	71.98	67.62	60.29	56.05	54.58	50.87
MMA [CVPR'24]	59.33	55.01	53.11	49.23	76.95	71.62	72.10	67.09	60.31	55.62	54.60	50.42
MAIL [Ours]	**60.11**	**57.40**	**53.34**	**50.95**	**78.94**	**74.80**	**73.91**	**70.14**	**62.05**	**58.31**	**56.05**	**52.80**

enhance the synergy between the vision and language agent layers, we introduce a multi-modal agent layer coupling approach. Specifically, the scaling vector a_v in the vision agent layer is integrated with a_t via a bottleneck-based language-to-vision projection, acting as a bridge function that facilitates gradient exchange and promotes aligned updates across the modalities:

$$\bar{a}_v = a_v + W_{up} \cdot W_{down} \cdot a_t, \tag{8}$$

where $W_{up} \in \mathbb{R}^{d_v \times r}$ or $W_{up} \in \mathbb{R}^{d_t \times r}$ and $W_{down} \in \mathbb{R}^{r \times d_t}$, with r representing the rank of the bridge function. Following the initialization method in LoRA [22], W_{down} is initialized with random Gaussian values, i.e., $W_{down} \sim \mathcal{N}(0, \sigma_t^2)$, with $\sigma_t = \frac{1}{\sqrt{d_t}}$, while W_{up} is initialized to zeros. $\bar{a}_v$ will replace in a_v in the image agent layer. **Alg. 1**, **2**, **3** provides the pseudo-codes for MAIL in a PyTorch-like style. With just a few lines, MAIL can significantly boost performance in a plug-and-play manner. Additional design details and variants are provided in **Appendix G**, including the structure of the bridge function, various initialization strategies, pseudocode, and other implementation choices.

4.3 Parameter Analysis

Here, we analyze the parameter complexity of MaPLe, MMA, and the proposed MAIL. For a transformer block, MAIL fine-tunes $(8 + 4r) \cdot (d_t + d_v)$ parameters, where r is set to 8 in our implementation for FS-UCDR. In contrast, MMA fine-tunes $2r_1 \cdot (d_t + d_v) + r_1^2$, with $r_1 = 32$ as the intermediate dimension of the bottleneck layer. Meanwhile, MaPLe requires $d_t d_v + N_p d_t$ parameters, with N_p denotes the number of text prompts. Based on these calculations, we conclude that MAIL and MMA have a comparable number of learnable parameters, while both are significantly more parameter-efficient than MaPLe, i.e., MAIL $\sim$ MMA $\ll$ MaPLe. The detailed time and resource consumption are provided in **Appendix E**.

5 Experiments

In this section, we evaluate the effectiveness of our proposed MAIL on two tasks: **FS-UCDR** (including its variants) and **few-shot classification.** Details on **datasets, metrics, implementations, loss functions and computational cost** are provided in **Appendix A, B, C, D, E**.

Table 2: FS-U^{D}CDR (2-shot) evaluation results (%) on DomainNet.

Methods	*Sketch*		*Quickdraw*		*Painting*		*Infograph*		*Clipart*		*Average*	
	mAP_{200}	$Prec_{200}$	mAP_{200}	$Prec_{200}$	mAP_{200}	$Prec_{200}$	mAP_{200}	$Prec_{200}$	mAP_{200}	$Prec_{200}$	mAP_{200}	$Prec_{200}$
ProS* [CVPR'24]	73.85	49.11	28.89	11.86	72.27	46.15	60.56	39.62	81.05	52.98	63.32	39.94
CLIP [ICML'21]	47.60	28.71	8.67	4.50	55.69	31.70	47.56	29.36	55.81	31.10	43.07	25.07
BitFit [ACL'22]	70.20	45.00	22.75	9.52	68.54	41.66	59.77	38.51	75.17	47.09	59.29	36.36
LoRA [ICLR'22]	58.01	62.05	39.23	17.67	7.34	65.72	38.90	57.94	35.52	41.77	54.59	32.55
VPT-D [ECCV'22]	65.63	42.96	22.33	10.01	66.66	41.13	57.63	37.20	73.64	46.46	57.18	35.55
AFormer [NeurIPS'22]	66.28	39.91	20.66	7.88	64.77	37.21	59.55	36.70	70.51	52.16	56.35	34.77
IVLP [CVPR'23]	64.54	42.17	21.31	9.51	66.55	40.58	59.26	37.64	72.31	44.80	56.79	34.94
IVLA [CVPR'24]	66.58	40.18	21.44	8.20	64.84	37.31	58.42	37.58	70.66	42.29	56.39	33.11
MaPLe [CVPR'23]	71.18	46.65	26.48	11.28	70.72	44.64	60.24	39.40	77.47	49.15	61.22	38.22
MMA [CVPR'24]	71.14	45.54	24.03	10.17	68.66	41.53	59.52	36.74	75.92	46.38	59.86	36.07
MAIL [Ours]	**73.61**	**49.20**	**26.91**	**11.60**	**72.53**	**45.93**	**62.69**	**41.35**	**79.81**	**52.21**	**63.11**	**40.06**

5.1 Experimental Setup for FS-UCDR and Its Variants

In terms of the retrieval task, we conduct three core evaluations to comprehensively assess MAIL's performance: FS-UCDR, FS-U^{D}CDR, and FS-U^{C}CDR. All experiments utilize a 2-shot setting, i.e., only $2\times N_S$ training examples per category, where N_S denotes the number of source domains.

Datasets. We conduct experiments on three benchmark datasets: DomainNet [38], Sketchy [41, 32], and TU-Berlin [12, 53]. DomainNet is utilized for FS-UCDR and FS-U^{D}CDR evaluations, while the Sketchy and TU-Berlin datasets are employed for FS-U^{C}CDR evaluation.

Table 3: FS-U^{C}CDR (2-shot) evaluation results (%) on Sketchy and TU-Berlin.

Methods	**Sketchy**		**TU-Berlin**	
	mAP_{200}	$Prec_{200}$	mAP_{all}	$Prec_{100}$
ProS* [CVPR'24]	69.91	65.45	66.75	74.42
CLIP [ICML'21]	35.82	33.08	31.45	46.12
BitFit [ACL'22]	67.71	64.01	65.51	73.68
LoRA [ICLR'22]	54.23	52.77	57.78	67.97
VPT-D [ECCV'22]	65.19	61.16	62.12	70.89
AFormer [NeurIPS'21]	56.87	52.31	58.95	70.14
IVLP [CVPR'23]	60.27	55.75	59.13	68.58
IVLA [CVPR'24]	56.77	52.71	59.13	70.42
MaPLe [CVPR'23]	71.86	68.14	65.90	73.73
MMA [CVPR'24]	61.59	57.14	63.70	72.69
MAIL [Ours]	**73.46**	**69.73**	**67.97**	**75.10**

Baselines. We primarily compare our methods with the following categories: ❶ adapter-based methods, including AdaptFormer (vision-only adapter) [6], IVLA (modality-independent adapter) [49], and MMA [49]; ❷ prompt-based methods, including VPT-D (vision-only prompt) [23], IVLP (modality-independent prompt) [24], and MaPLe [24]; ❸ partially fine-tuned methods, including LoRA [22] and BitFit [52]; ❹ other methods, including the zero-shot CLIP [39] and the SOTA method under UCDR, ProS [13]. Implementation details of these methods are provided in **Appendix F**.

5.2 Experimental Setup for Few-Shot Classification

We also conduct three core few-shot classification evaluations that are widely adopted in prior work: ❶ base-to-novel generalization, ❷ cross-dataset evaluation, and ❸ domain generalization. All experiments are conducted under a 16-shot setting, i.e., using 16 training examples per category.

Datasets. We conduct the base-to-novel generalization and cross-dataset evaluations across 11 diverse image classification datasets: ImageNet [9], Caltech101 [14], OxfordPets [36], StanfordCars [29], Flowers102 [34], Food101 [2], FGVCAircraft [33], SUN397 [48], UCF101 [35], DTD [8], and EuroSAT [17]. In terms of the domain generalization evaluation, we use ImageNet as the training dataset and evaluate on four variants—ImageNetV2 [40], ImageNet-Sketch [46], ImageNet-A [19], and ImageNet-R [18]—each introducing different types of domain variation.

Baselines. We primarily compare our method with prompt-based and adapter-based approaches, including CoOp [57], CoCoOp [56], MaPLe [24], and MMA [49], as well as regularization-based methods such as KgCoOp [50], PromptSRC [25], and DeKg [30]. To ensure fairness, we exclude methods that rely on LLMs or adopt regularization purely as an auxiliary loss trick.

5.3 Comparison Results

Comparison Results under FS-UCDR and FS-U^{D}CDR. We compare the FS-UCDR and FS-U^{D}CDR performance of our MAIL against other baselines on DomainNet, as summarized in **Tab. 1** and **Tab. 2**. We identify several key observations: ❶ *Our method consistently outperforms existing baselines.* Notably, under FS-UCDR, MAIL significantly outperforms ProS, a model operate under data-efficient UCDR. Moreover, MAIL achieves comparable performance under FS-U^{D}CDR while

Table 4: Base-to-novel generalization (16-shot) evaluation results (%) across 11 datasets.

Methods	***Average***			ImageNet			Caltech101			OxfordPets		
	Base	Novel	HM	Base	Novel	HM	Base	Novel	HM	Base	Novel	HM
CLIP [ICML'21]	69.34	74.22	71.70	72.43	68.14	70.22	96.84	94.00	95.40	91.17	97.26	94.12
CoOp [IJCV'22]	82.69	63.22	71.66	76.47	67.88	71.92	98.00	89.81	93.73	93.67	95.29	94.47
CoOpOp [CVPR'22]	80.47	71.69	75.83	75.98	70.43	73.10	97.96	93.81	95.84	95.20	97.69	96.43
KgCoOp [CVPR'23]	80.73	73.60	77.00	75.83	69.96	72.78	97.72	94.39	96.03	94.65	97.76	96.18
MaPLe [CVPR'21]	82.28	75.14	78.55	76.66	70.54	73.47	97.74	94.36	96.02	95.43	97.76	96.58
PromptSRC [ICCV'23]	84.26	76.10	79.97	77.60	70.73	74.01	98.10	94.03	96.02	95.33	97.30	96.30
MMA [CVPR'24]	83.20	76.80	79.87	77.31	71.00	74.02	98.40	94.00	96.15	95.40	**98.07**	96.72
DeKg [ICLR'25]	84.96	76.38	80.44	77.40	69.20	73.07	**98.64**	95.20	**96.89**	94.47	97.76	96.09
MAIL [Ours]	**85.19**	**77.39**	**81.10**	**77.92**	**71.22**	**74.42**	98.34	**95.36**	96.83	**95.50**	97.97	**96.72**

Methods	StanfordCars			Flowers102			Food101			FGVCAircraft		
	Base	Novel	HM	Base	Novel	HM	Base	Novel	HM	Base	Novel	HM
CLIP [ICML'21]	63.37	74.89	68.65	72.08	77.80	74.83	90.10	91.22	90.66	27.19	36.29	31.09
CoOp [IJCV'22]	78.12	60.40	68.13	97.60	59.67	74.06	88.33	82.26	85.19	40.44	22.30	28.75
CoOpOp [CVPR'22]	70.49	73.59	72.01	94.87	71.75	81.71	90.70	91.29	90.99	33.41	23.71	27.74
KgCoOp [CVPR'22]	71.76	**75.04**	73.36	95.00	74.73	83.65	90.50	91.70	91.09	36.21	33.55	34.83
MaPLe [CVPR'23]	72.94	74.00	73.47	95.92	72.46	82.56	90.71	**92.05**	**91.38**	37.44	35.61	36.50
PromptSRC [ICCV'23]	78.27	74.97	76.58	98.07	**76.50**	**85.95**	90.67	91.53	91.10	42.73	**37.87**	40.15
MMA [CVPR'24]	78.50	73.10	75.70	97.77	75.93	85.48	90.13	91.30	90.71	40.57	36.33	38.33
DeKg [ICLR'25]	81.18	74.75	**77.83**	**98.58**	75.18	85.30	**90.73**	91.55	91.14	45.20	35.09	39.51
MAIL [Ours]	**82.27**	72.03	76.81	98.20	75.27	85.22	90.54	91.77	91.15	**47.80**	36.27	**41.24**

Method	SUN397			DTD			EuroSAT			UCF101		
	Base	Novel	HM	Base	Novel	HM	Base	Novel	HM	Base	Novel	HM
CLIP [ICML'21]	69.36	75.35	72.23	53.24	59.90	56.37	56.48	64.05	60.03	70.53	77.50	73.85
CoOp [IJCV'22]	80.60	65.89	72.51	79.44	41.18	54.24	92.19	54.74	68.69	84.69	56.05	67.46
CoOpOp [CVPR'22]	79.74	76.86	78.27	77.01	56.00	64.85	87.49	60.04	71.21	82.33	73.45	77.64
KgCoOp [CVPR'22]	80.29	76.53	78.36	77.55	54.99	64.35	85.64	64.34	73.48	82.89	76.67	79.65
MaPLe [CVPR'23]	80.82	78.70	79.75	80.36	59.18	68.16	**94.07**	73.23	82.35	83.00	78.66	80.77
PromptSRC [ICCV'23]	**82.67**	78.47	80.52	83.37	62.97	71.75	92.90	73.90	82.32	87.10	78.80	82.74
MMA [CVPR'24]	82.27	78.57	80.38	83.20	65.63	73.38	85.46	82.34	83.87	86.23	80.03	82.20
DeKg [ICLR'25]	82.52	78.30	80.35	**83.80**	59.66	69.70	94.02	81.69	87.42	**88.06**	**81.77**	**84.80**
MAIL [Ours]	82.50	**78.70**	**80.56**	83.15	**67.39**	**74.45**	93.50	**85.11**	**89.11**	87.34	80.22	83.63

utilizing only approximately 1/140 of ProS's training data, highlighting its remarkable efficiency in low-data scenarios. ❷ *Modality-coupled methods consistently outperform modality independent methods.* For instance, under FS-UCDR's UnseenGallery scenario, MaPLe and MMA achieve average mAP_{200} improvements of 4.44% and 3.22% over IVLP and IVLA, respectively. This emphasizes the importance of collaboration and information sharing between modalities in low-data settings. ❸ *The vision-only methods perform similarly to, or even slightly outperform, the modality-independent methods.* As seen in the table, AdaptFormer achieves results comparable to IVLA, while VPT-Deep achieves an average mAP improvement of 0.5%-1.6% over IVLP. Therefore, we conclude that the benefit of simply fine-tuning the text side for retrieval is limited.

Comparison Results under FS-U^{C}CDR. In **Tab. 3**, we compare the FS-U^{C}CDR performance of our MAIL with other baselines. The results demonstrate that MAIL consistently achieves the best performance among all methods, indicating its effectiveness in enhancing CLIP's capability to handle semantic shifts under limited-data scenarios. Moreover, it can be observed that adapter-based methods and LoRA perform relatively poorly under the FS-U^{C}CDR setting.

Comparison Results under Few-Shot Classification. In **Tab. 4**, we compare the base-to-novel performance of MAIL against existing baselines across 11 datasets, reporting accuracies on base and novel classes, along with their harmonic mean (HM). Without relying on any regularization loss, MAIL achieves consistent gains of 0.23%, 1.01%, and 0.66% in Base, Novel, and HM, respectively, surpassing the previous best method, DeKg [30]. The improvement on novel classes is particularly notable, as DeKg [30] depends on regularization to enhance generalization, while MAIL attains better results with a simpler, regularization-free design. For results under the other two evaluation settings, please refer to **Tab. 5** and **Tab. 6**, where our MAIL also showcases strong performance.

5.4 Ablation Studies

In this section, we assess the performance of each component within MAIL. By default, we present the *average performance* scores for the UnseenGallery and MixedGallery scenarios on DomainNet across five query domains under FS-UCDR. More ablation studies can be found in **Appendix G, H**.

Table 5: Comparison of MAIL with previous state-of-the-art methods on cross-dataset evaluation.

	Source	Target									
	ImageNet	Average	Caltech101	OxfordPets	StanfordCars	Flowers101	Food101	FGVCAircraft	SUN397	DTD	EuroSAT	UCF101
CoOp [IJCV'22]	71.51	63.88	93.70	89.14	64.51	68.71	85.30	18.47	64.15	41.92	46.39	66.55
CoOpOp [CVPR'22]	71.02	65.74	94.43	90.14	65.32	71.88	86.06	22.94	67.36	45.73	45.37	68.21
MaPLe [CVPR'23]	70.72	66.30	93.53	90.49	65.57	72.23	86.20	24.74	67.01	46.49	48.06	68.69
PromptSRC [ICCV'23]	71.27	65.81	93.60	90.25	65.70	70.25	86.15	23.90	67.10	**46.87**	45.50	68.75
MMA [CVPR'24]	71.00	66.61	93.80	90.30	66.13	72.07	86.12	**25.33**	**68.17**	46.57	49.24	68.32
DeKg[ICLR'25]	**72.33**	66.64	**94.73**	90.02	65.49	**72.39**	**86.59**	25.05	67.19	44.47	51.37	68.78
MAIL [Ours]	72.10	**67.02**	**94.73**	**91.37**	**66.63**	71.47	86.33	25.27	67.30	45.47	**52.80**	**68.87**

Table 6: Comparison of MAIL with previous state-of-the-art methods on domain generalization across 4 datasets. These results of DeKg are derived from their OpenReview comment section.

	Source	Target				
	ImageNet	Average	-V2	-S	-A	-R
CLIP [ICML'21]	66.73	57.17	60.83	46.15	47.77	73.96
CoOp [IJCV'22]	71.51	59.27	64.20	47.99	49.71	75.21
CoOpOp [CVPR'22]	71.02	59.91	64.07	48.75	50.63	76.18
MaPLe [CVPR'23]	70.72	60.28	64.07	49.15	50.90	76.98
PromptSRC [ICCV'23]	71.27	60.65	64.35	49.55	50.90	**77.80**
MMA CVPR'24]	71.00	60.47	64.33	49.13	**51.12**	77.32
DeKg [ICLR'25]	**72.33**	59.89	64.31	48.38	50.51	76.37
MAIL [Ours]	72.10	**60.68**	**64.50**	**49.67**	50.70	**77.80**

Table 7: Ablation studies on variants of AL and MAIL.

Methods	**UnseenGallery**		**MixedGallery**		**Params.** (↓)
	mAP_{200}	$Prec_{200}$	mAP_{all}	$Prec_{100}$	
VU	59.13	54.59	53.34	49.24	**76288**
IVLU	58.88	54.29	53.13	49.06	127488
V → L	58.67	54.00	52.97	48.79	637400
V ↔ L	61.75	58.07	55.83	52.58	1147392
V ← L	**62.05**	**58.31**	**56.05**	**52.80**	637400

Variants of AL and MAIL. We first compare the performance of adding ALs to both encoders (IVLU) versus only to the image encoder (VU), as shown in the first two rows of **Tab. 7**, focusing exclusively on the image encoder yields better results. Next, we analyze the directionality of information flow in MAIL. Vision-to-language flow ($V \rightarrow L$) reduces the model's representational capacity, as evidenced by its poorer performance compared to IVLU. Similarly, the bidirectional flow ($V \leftrightarrow L$) underperforms compared to language-guided alignment ($L \leftarrow V$). This is likely due to visual features, which often include significant background noise and limited category-specific information, diluting the discriminability of text features. In contrast, text features, being semantically compact and category-specific, are better suited to guide alignment effectively without being adversely affected by redundant noisy information.

Variants of Adding AL. We begin by evaluating the effect of placing ALs at the final LN and projection layers of both encoders, as shown in **Fig. 4-a**. Results reveal a significant performance boost when ALs are applied to these locations. Please note that when we add AL to the projection layer, we also set the projection layer trainable. Next, we progressively distribute ALs across transformer blocks, from the first layer to the l-th block ($l = 1, 2, \ldots, 12$). As shown in **Fig. 4-b**, performance peaks when ALs are added to all 12 layers. Furthermore, we examine the effect of removing ALs from key transformer components—MLP, attention, and LN layers. **Fig. 4-c** shows that stepwise removal consistently degrades performance, highlighting the critical role of ALs across all components.

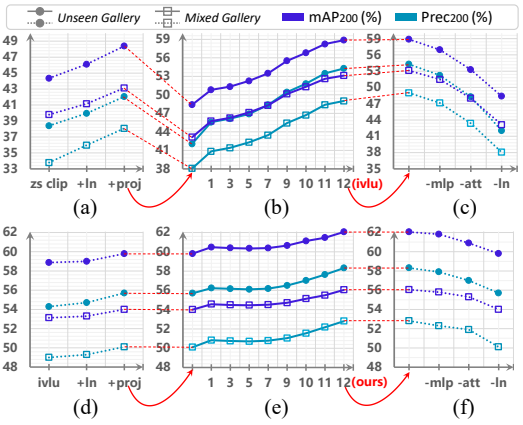

Figure 4: Ablation studies on different configurations of adding AL and MAIL.

Variants of Adding MAIL. Building on IVLU, we integrate the bottleneck-based bridge function into ALs, transforming them into MAILs. We first place the bridge function in the final LN and projection layers of both encoders, as illustrated in **Fig. 4-d**, which delivers promising results. Next, we incrementally add the bridge function to ALs in each transformer block, as shown in **Fig. 4-e**. Notably, introducing the bridge function in the first block yields a significant performance boost. While subsequent additions initially cause minor declines, a sharp improvement begins at the 10th block, culminating in the best performance when applied across all 12 blocks. Finally, we remove the bridge function (degrading MAIL to AL) systematically from each transformer block. **Fig. 4-f** reveals that removing it from the LN layer has the most pronounced negative effect.

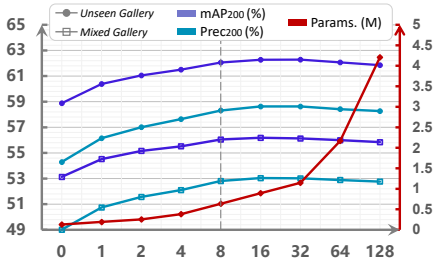

Figure 5: Ablation studies on different ranks. $rank = 0$ denotes IVLU.

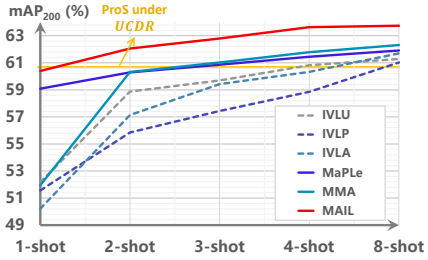

Figure 6: Results with different shots under FS-UCDR (UnseenGallery).

Rank of the Bridge Function. To evaluate the impact the rank of the bridge function in our MAIL, we conduct an ablation study by varying the rank systematically. As shown in **Fig. 5**, performance peaks when the rank is set to 16. However, increasing the rank beyond 16 leads to a slight decline in performance, likely due to the additional parameters increasing the risk of overfitting. To achieve a better trade-off, we select a rank of 8 for the final configuration.

Results with Different Shots. Fig. 6 presents the results of our method compared to other methods across varying shot numbers, with detailed numerical values provided in **Appendix I**. This figure clearly demonstrates that the performance of all methods improves as the number of shots increases. Notably, our method consistently outperforms the its competitors. Additionally, it is worth noting that nearly all methods surpass ProS [13] with proper shots.

6 Conclusion and Limitation

In this paper, we introduce FS-UCDR, a practical setting that alleviates the data scarcity challenge in UCDR. Accordingly, we propose MAIL, a novel approach that enhances update alignment between modalities through coupled agent layers. Leveraging a scaling-and-shifting reparameterization mechanism, these agent layers are seamlessly integrated into the original CLIP, preserving inference efficiency while improving adaptability. Extensive experiments across three benchmarks validate its effectiveness. Beyond retrieval, MAIL's alignment strategy also holds promise for few-shot classification.

The **limitation** of MAIL lies in: MAIL's sequential nature, i.e., $\mathrm{AL} \circ \mathrm{OP}(x)$ leads to slight longer training time and memory (as we have provided in the **Appendix E**) compared with MaPLe and MMA. We will explore optimizations in future work.

7 Acknowledgments and Disclosure of Funding

This work was supported by the National Natural Science Foundation of China (Nos. 62476056 and 62306070) and the Social Development Science and Technology Project of Jiangsu Province (No. BE2022811). This work was also supported in part by the Southeast University Start-Up Grant for New Faculty under Grant 4009002309. Furthermore, the work was supported by the Big Data Computing Center of Southeast University and the SEU Innovation Capability Enhancement Plan for Doctoral Student (CXJH_SEU 25133). This work was also supported by "the Fundamental Research Funds for the Central Universities (2242025K30024)".

References

[1] Samyadeep Basu, Shell Hu, Daniela Massiceti, and Soheil Feizi. Strong baselines for parameter-efficient few-shot fine-tuning. In *Proceedings of the AAAI Conference on Artificial Intelligence*, volume 38, pages 11024–11031, 2024.

[2] Lukas Bossard, Matthieu Guillaumin, and Luc Van Gool. Food-101–mining discriminative components with random forests. In *Computer vision–ECCV 2014: 13th European conference, zurich, Switzerland, September 6-12, 2014, proceedings, part VI 13*, pages 446–461. Springer, 2014.

[3] Kaixiang Chen, Pengfei Fang, and Hui Xue. Depro: Domain ensemble using decoupled prompts for universal cross-domain retrieval. In *Proceedings of the 48th International ACM SIGIR Conference on Research and Development in Information Retrieval*, SIGIR '25, page 958–967, 2025.

[4] Kaixiang Chen, Pengfei Fang, Zi Ye, and Liyan Zhang. Multi-scale explicit matching and mutual subject teacher learning for generalizable person re-identification. *IEEE Transactions on Circuits and Systems for Video Technology*, 34(9):8881–8895, 2024.

[5] Kaixiang Chen, Tiantian Gong, and Liyan Zhang. Camera-aware recurrent learning and earth mover's test-time adaption for generalizable person re-identification. *IEEE Transactions on Circuits and Systems for Video Technology*, 34(1):357–370, 2024.

[6] Shoufa Chen, Chongjian Ge, Zhan Tong, Jiangliu Wang, Yibing Song, Jue Wang, and Ping Luo. Adaptformer: Adapting vision transformers for scalable visual recognition. In *Advances in Neural Information Processing Systems*, volume 35, pages 16664–16678, 2022.

[7] Xiaohong Chen, Canran Xiao, and Yongmei Liu. Confusion-resistant federated learning via diffusion-based data harmonization on non-iid data. In *The Thirty-eighth Annual Conference on Neural Information Processing Systems*, pages 137495–137520, 2024.

[8] Mircea Cimpoi, Subhransu Maji, Iasonas Kokkinos, Sammy Mohamed, and Andrea Vedaldi. Describing textures in the wild. In *Proceedings of the IEEE conference on computer vision and pattern recognition*, pages 3606–3613, 2014.

[9] Jia Deng, Wei Dong, Richard Socher, Li-Jia Li, Kai Li, and Li Fei-Fei. Imagenet: A large-scale hierarchical image database. In *2009 IEEE conference on computer vision and pattern recognition*, pages 248–255. Ieee, 2009.

[10] Jacob Devlin, Ming-Wei Chang, Kenton Lee, and Kristina Toutanova. BERT: pre-training of deep bidirectional transformers for language understanding. In *Proceedings of the 2019 Conference of the North American Chapter of the Association for Computational Linguistics*, pages 4171–4186, 2019.

[11] Alexey Dosovitskiy, Lucas Beyer, Alexander Kolesnikov, Dirk Weissenborn, Xiaohua Zhai, Thomas Unterthiner, Mostafa Dehghani, Matthias Minderer, Georg Heigold, Sylvain Gelly, Jakob Uszkoreit, and Neil Houlsby. An image is worth 16x16 words: Transformers for image recognition at scale. In *9th International Conference on Learning Representations, ICLR*, 2021.

[12] Mathias Eitz, James Hays, and Marc Alexa. How do humans sketch objects? *ACM Transactions on graphics (TOG)*, 31(4):1–10, 2012.

[13] Kaipeng Fang, Jingkuan Song, Lianli Gao, Pengpeng Zeng, Zhi-Qi Cheng, Xiyao Li, and Heng Tao Shen. Pros: Prompting-to-simulate generalized knowledge for universal cross-domain retrieval. In *Proceedings of the IEEE/CVF Conference on Computer Vision and Pattern Recognition*, pages 17292–17301, 2024.

[14] Li Fei-Fei, Rob Fergus, and Pietro Perona. Learning generative visual models from few training examples: An incremental bayesian approach tested on 101 object categories. In *2004 conference on computer vision and pattern recognition workshop*, pages 178–178. IEEE, 2004.

[15] Peng Gao, Shijie Geng, Renrui Zhang, Teli Ma, Rongyao Fang, Yongfeng Zhang, Hongsheng Li, and Yu Qiao. Clip-adapter: Better vision-language models with feature adapters. *International Journal of Computer Vision*, 132(2):581–595, 2024.

[16] Ce Ge, Jingyu Wang, Qi Qi, Haifeng Sun, Tong Xu, and Jianxin Liao. Scene-level sketch-based image retrieval with minimal pairwise supervision. In *Proceedings of the AAAI Conference on Artificial Intelligence*, pages 650–657, 2023.

[17] Patrick Helber, Benjamin Bischke, Andreas Dengel, and Damian Borth. Eurosat: A novel dataset and deep learning benchmark for land use and land cover classification. *IEEE Journal of Selected Topics in Applied Earth Observations and Remote Sensing*, 12(7):2217–2226, 2019.

[18] Dan Hendrycks, Steven Basart, Norman Mu, Saurav Kadavath, Frank Wang, Evan Dorundo, Rahul Desai, Tyler Zhu, Samyak Parajuli, Mike Guo, et al. The many faces of robustness: A critical analysis of out-of-distribution generalization. In *Proceedings of the IEEE/CVF international conference on computer vision*, pages 8340–8349, 2021.

[19] Dan Hendrycks, Kevin Zhao, Steven Basart, Jacob Steinhardt, and Dawn Song. Natural adversarial examples. In *Proceedings of the IEEE/CVF conference on computer vision and pattern recognition*, pages 15262–15271, 2021.

[20] Alexander Hermans, Lucas Beyer, and Bastian Leibe. In defense of the triplet loss for person re-identification, 2017.

[21] Neil Houlsby, Andrei Giurgiu, Stanislaw Jastrzebski, Bruna Morrone, Quentin De Laroussilhe, Andrea Gesmundo, Mona Attariyan, and Sylvain Gelly. Parameter-efficient transfer learning for nlp. In *International conference on machine learning*, pages 2790–2799. PMLR, 2019.

[22] Edward J. Hu, Yelong Shen, Phillip Wallis, Zeyuan Allen-Zhu, Yuanzhi Li, Shean Wang, Lu Wang, and Weizhu Chen. Lora: Low-rank adaptation of large language models. In *The Tenth International Conference on Learning Representations, ICLR*, 2022.

[23] Menglin Jia, Luming Tang, Bor-Chun Chen, Claire Cardie, Serge Belongie, Bharath Hariharan, and Ser-Nam Lim. Visual prompt tuning. In *European Conference on Computer Vision*, pages 709–727. Springer, 2022.

[24] Muhammad Uzair Khattak, Hanoona Rasheed, Muhammad Maaz, Salman Khan, and Fahad Shahbaz Khan. Maple: Multi-modal prompt learning. In *Proceedings of the IEEE/CVF Conference on Computer Vision and Pattern Recognition*, pages 19113–19122, 2023.

[25] Muhammad Uzair Khattak, Syed Talal Wasim, Muzammal Naseer, Salman Khan, Ming-Hsuan Yang, and Fahad Shahbaz Khan. Self-regulating prompts: Foundational model adaptation without forgetting. In *Proceedings of the IEEE/CVF International Conference on Computer Vision*, pages 15190–15200, 2023.

[26] Subhadeep Koley, Ayan Kumar Bhunia, Aneeshan Sain, Pinaki Nath Chowdhury, Tao Xiang, and Yi-Zhe Song. How to handle sketch-abstraction in sketch-based image retrieval? In *Proceedings of the IEEE/CVF Conference on Computer Vision and Pattern Recognition*, pages 16859–16869, 2024.

[27] Dawid Jan Kopiczko, Tijmen Blankevoort, and Yuki M. Asano. Vera: Vector-based random matrix adaptation. In *The Twelfth International Conference on Learning Representations, ICLR*, 2024.

[28] Simon Kornblith, Jonathon Shlens, and Quoc V Le. Do better imagenet models transfer better? In *Proceedings of the IEEE/CVF conference on computer vision and pattern recognition*, pages 2661–2671, 2019.

[29] Jonathan Krause, Michael Stark, Jia Deng, and Li Fei-Fei. 3d object representations for fine-grained categorization. In *Proceedings of the IEEE international conference on computer vision workshops*, pages 554–561, 2013.

[30] Yilun Li, Miaomiao Cheng, Xu Han, and Wei Song. Divergence-enhanced knowledge-guided context optimization for visual-language prompt tuning. In *The Thirteenth International Conference on Learning Representations*, 2025.

[31] Dongze Lian, Daquan Zhou, Jiashi Feng, and Xinchao Wang. Scaling & shifting your features: A new baseline for efficient model tuning. In *Advances in Neural Information Processing Systems (NeurIPS)*, 2022.

[32] Li Liu, Fumin Shen, Yuming Shen, Xianglong Liu, and Ling Shao. Deep sketch hashing: Fast free-hand sketch-based image retrieval. In *Proceedings of the IEEE conference on computer vision and pattern recognition*, pages 2862–2871, 2017.

[33] Subhransu Maji, Esa Rahtu, Juho Kannala, Matthew Blaschko, and Andrea Vedaldi. Fine-grained visual classification of aircraft. *arXiv preprint arXiv:1306.5151*, 2013.

[34] Maria-Elena Nilsback and Andrew Zisserman. Automated flower classification over a large number of classes. In *2008 Sixth Indian conference on computer vision, graphics & image processing*, pages 722–729. IEEE, 2008.

[35] Maria-Elena Nilsback and Andrew Zisserman. Automated flower classification over a large number of classes. In *2008 Sixth Indian conference on computer vision, graphics & image processing*, pages 722–729. IEEE, 2008.

[36] Omkar M Parkhi, Andrea Vedaldi, Andrew Zisserman, and CV Jawahar. Cats and dogs. In *2012 IEEE conference on computer vision and pattern recognition*, pages 3498–3505. IEEE, 2012.

[37] Soumava Paul, Titir Dutta, and Soma Biswas. Universal cross-domain retrieval: Generalizing across classes and domains. In *Proceedings of the IEEE/CVF International Conference on Computer Vision*, pages 12056–12064, 2021.

[38] Xingchao Peng, Qinxun Bai, Xide Xia, Zijun Huang, Kate Saenko, and Bo Wang. Moment matching for multi-source domain adaptation. In *Proceedings of the IEEE/CVF international conference on computer vision*, pages 1406–1415, 2019.

[39] Alec Radford, Jong Wook Kim, Chris Hallacy, Aditya Ramesh, Gabriel Goh, Sandhini Agarwal, Girish Sastry, Amanda Askell, Pamela Mishkin, Jack Clark, et al. Learning transferable visual models from natural language supervision. In *International conference on machine learning*, pages 8748–8763. PMLR, 2021.

[40] Benjamin Recht, Rebecca Roelofs, Ludwig Schmidt, and Vaishaal Shankar. Do imagenet classifiers generalize to imagenet? In *International conference on machine learning*, pages 5389–5400. PMLR, 2019.

[41] Patsorn Sangkloy, Nathan Burnell, Cusuh Ham, and James Hays. The sketchy database: learning to retrieve badly drawn bunnies. *ACM Transactions on Graphics (TOG)*, 35(4):1–12, 2016.

[42] Marvin Teichmann, Andre Araujo, Menglong Zhu, and Jack Sim. Detect-to-retrieve: Efficient regional aggregation for image search. In *Proceedings of the IEEE/CVF Conference on Computer Vision and Pattern Recognition*, pages 5109–5118, 2019.

[43] Jialin Tian, Xing Xu, Kai Wang, Zuo Cao, Xunliang Cai, and Heng Tao Shen. Structure-aware semantic-aligned network for universal cross-domain retrieval. In *Proceedings of the 45th International ACM SIGIR Conference on Research and Development in Information Retrieval*, pages 278–289, 2022.

[44] Laurens Van der Maaten and Geoffrey Hinton. Visualizing data using t-sne. *Journal of machine learning research*, 9(11), 2008.

[45] Ashish Vaswani, Noam Shazeer, Niki Parmar, Jakob Uszkoreit, Llion Jones, Aidan N. Gomez, Lukasz Kaiser, and Illia Polosukhin. Attention is all you need. In *Advances in Neural Information Processing Systems*, volume 30, pages 5998–6008, 2017.

[46] Haohan Wang, Songwei Ge, Zachary Lipton, and Eric P Xing. Learning robust global representations by penalizing local predictive power. *Advances in Neural Information Processing Systems*, 32, 2019.

[47] Tobias Weyand, Andre Araujo, Bingyi Cao, and Jack Sim. Google landmarks dataset v2-a large-scale benchmark for instance-level recognition and retrieval. In *Proceedings of the IEEE/CVF conference on computer vision and pattern recognition*, pages 2575–2584, 2020.

[48] Jianxiong Xiao, James Hays, Krista A Ehinger, Aude Oliva, and Antonio Torralba. Sun database: Large-scale scene recognition from abbey to zoo. In *2010 IEEE computer society conference on computer vision and pattern recognition*, pages 3485–3492. IEEE, 2010.

[49] Lingxiao Yang, Ru-Yuan Zhang, Yanchen Wang, and Xiaohua Xie. Mma: Multi-modal adapter for vision-language models. In *Proceedings of the IEEE/CVF Conference on Computer Vision and Pattern Recognition*, pages 23826–23837, 2024.

[50] Hantao Yao, Rui Zhang, and Changsheng Xu. Visual-language prompt tuning with knowledge-guided context optimization. In *Proceedings of the IEEE/CVF Conference on Computer Vision and Pattern Recognition*, pages 6757–6767, 2023.

[51] Jiawei Yao, Chuming Li, and Canran Xiao. Swift sampler: Efficient learning of sampler by 10 parameters. In *The Thirty-eighth Annual Conference on Neural Information Processing Systems*, pages 59030–59053, 2024.

[52] Elad Ben Zaken, Yoav Goldberg, and Shauli Ravfogel. Bitfit: Simple parameter-efficient fine-tuning for transformer-based masked language-models. In Smaranda Muresan, Preslav Nakov, and Aline Villavicencio, editors, *Proceedings of the 60th Annual Meeting of the Association for Computational Linguistics*, pages 1–9, 2022.

[53] Hua Zhang, Si Liu, Changqing Zhang, Wenqi Ren, Rui Wang, and Xiaochun Cao. Sketchnet: Sketch classification with web images. In *Proceedings of the IEEE conference on computer vision and pattern recognition*, pages 1105–1113, 2016.

[54] Renrui Zhang, Xiangfei Hu, Bohao Li, Siyuan Huang, Hanqiu Deng, Yu Qiao, Peng Gao, and Hongsheng Li. Prompt, generate, then cache: Cascade of foundation models makes strong few-shot learners. In *Proceedings of the IEEE/CVF Conference on Computer Vision and Pattern Recognition*, pages 15211–15222, 2023.

[55] Renrui Zhang, Wei Zhang, Rongyao Fang, Peng Gao, Kunchang Li, Jifeng Dai, Yu Qiao, and Hongsheng Li. Tip-adapter: Training-free adaption of clip for few-shot classification. In *European conference on computer vision*, pages 493–510. Springer, 2022.

[56] Kaiyang Zhou, Jingkang Yang, Chen Change Loy, and Ziwei Liu. Conditional prompt learning for vision-language models. In *Proceedings of the IEEE/CVF conference on computer vision and pattern recognition*, pages 16816–16825, 2022.

[57] Kaiyang Zhou, Jingkang Yang, Chen Change Loy, and Ziwei Liu. Learning to prompt for vision-language models. *International Journal of Computer Vision*, 130(9):2337–2348, 2022.

NeurIPS Paper Checklist

1. **Claims**

   Question: Do the main claims made in the abstract and introduction accurately reflect the paper's contributions and scope?

   Answer: [Yes]

   Justification: The abstract and introduction clearly state the claims made.

   Guidelines:

   - The answer NA means that the abstract and introduction do not include the claims made in the paper.
   - The abstract and/or introduction should clearly state the claims made, including the contributions made in the paper and important assumptions and limitations. A No or NA answer to this question will not be perceived well by the reviewers.
   - The claims made should match theoretical and experimental results, and reflect how much the results can be expected to generalize to other settings.
   - It is fine to include aspirational goals as motivation as long as it is clear that these goals are not attained by the paper.

2. **Limitations**

   Question: Does the paper discuss the limitations of the work performed by the authors?

   Answer: [Yes]

   Justification: The limitation of our method is the slightly higher computational cost during training compared to other PEFT methods.

   Guidelines:

   - The answer NA means that the paper has no limitation while the answer No means that the paper has limitations, but those are not discussed in the paper.
   - The authors are encouraged to create a separate "Limitations" section in their paper.
   - The paper should point out any strong assumptions and how robust the results are to violations of these assumptions (e.g., independence assumptions, noiseless settings, model well-specification, asymptotic approximations only holding locally). The authors should reflect on how these assumptions might be violated in practice and what the implications would be.
   - The authors should reflect on the scope of the claims made, e.g., if the approach was only tested on a few datasets or with a few runs. In general, empirical results often depend on implicit assumptions, which should be articulated.
   - The authors should reflect on the factors that influence the performance of the approach. For example, a facial recognition algorithm may perform poorly when image resolution is low or images are taken in low lighting. Or a speech-to-text system might not be used reliably to provide closed captions for online lectures because it fails to handle technical jargon.
   - The authors should discuss the computational efficiency of the proposed algorithms and how they scale with dataset size.
   - If applicable, the authors should discuss possible limitations of their approach to address problems of privacy and fairness.
   - While the authors might fear that complete honesty about limitations might be used by reviewers as grounds for rejection, a worse outcome might be that reviewers discover limitations that aren't acknowledged in the paper. The authors should use their best judgment and recognize that individual actions in favor of transparency play an important role in developing norms that preserve the integrity of the community. Reviewers will be specifically instructed to not penalize honesty concerning limitations.

3. **Theory assumptions and proofs**

   Question: For each theoretical result, does the paper provide the full set of assumptions and a complete (and correct) proof?

   Answer: [NA]

Justification: This paper does not include any theoretical results. Instead, it focuses on thorough experimental validation and strong empirical performance, which we believe are more appropriate and relevant for evaluating the proposed method.

Guidelines:

- The answer NA means that the paper does not include theoretical results.
- All the theorems, formulas, and proofs in the paper should be numbered and cross-referenced.
- All assumptions should be clearly stated or referenced in the statement of any theorems.
- The proofs can either appear in the main paper or the supplemental material, but if they appear in the supplemental material, the authors are encouraged to provide a short proof sketch to provide intuition.
- Inversely, any informal proof provided in the core of the paper should be complemented by formal proofs provided in appendix or supplemental material.
- Theorems and Lemmas that the proof relies upon should be properly referenced.

4. **Experimental result reproducibility**

   Question: Does the paper fully disclose all the information needed to reproduce the main experimental results of the paper to the extent that it affects the main claims and/or conclusions of the paper (regardless of whether the code and data are provided or not)?

   Answer: [Yes]

   Justification: We have spare no efforts to illustrate the implementation details.

   Guidelines:

   - The answer NA means that the paper does not include experiments.
   - If the paper includes experiments, a No answer to this question will not be perceived well by the reviewers: Making the paper reproducible is important, regardless of whether the code and data are provided or not.
   - If the contribution is a dataset and/or model, the authors should describe the steps taken to make their results reproducible or verifiable.
   - Depending on the contribution, reproducibility can be accomplished in various ways. For example, if the contribution is a novel architecture, describing the architecture fully might suffice, or if the contribution is a specific model and empirical evaluation, it may be necessary to either make it possible for others to replicate the model with the same dataset, or provide access to the model. In general. releasing code and data is often one good way to accomplish this, but reproducibility can also be provided via detailed instructions for how to replicate the results, access to a hosted model (e.g., in the case of a large language model), releasing of a model checkpoint, or other means that are appropriate to the research performed.
   - While NeurIPS does not require releasing code, the conference does require all submissions to provide some reasonable avenue for reproducibility, which may depend on the nature of the contribution. For example
     (a) If the contribution is primarily a new algorithm, the paper should make it clear how to reproduce that algorithm.
     (b) If the contribution is primarily a new model architecture, the paper should describe the architecture clearly and fully.
     (c) If the contribution is a new model (e.g., a large language model), then there should either be a way to access this model for reproducing the results or a way to reproduce the model (e.g., with an open-source dataset or instructions for how to construct the dataset).
     (d) We recognize that reproducibility may be tricky in some cases, in which case authors are welcome to describe the particular way they provide for reproducibility. In the case of closed-source models, it may be that access to the model is limited in some way (e.g., to registered users), but it should be possible for other researchers to have some path to reproducing or verifying the results.

5. **Open access to data and code**

Question: Does the paper provide open access to the data and code, with sufficient instructions to faithfully reproduce the main experimental results, as described in supplemental material?

Answer: [Yes]

Justification: We will provide the code if the paper is accepted.

Guidelines:

- The answer NA means that paper does not include experiments requiring code.
- Please see the NeurIPS code and data submission guidelines (https://nips.cc/public/guides/CodeSubmissionPolicy) for more details.
- While we encourage the release of code and data, we understand that this might not be possible, so "No" is an acceptable answer. Papers cannot be rejected simply for not including code, unless this is central to the contribution (e.g., for a new open-source benchmark).
- The instructions should contain the exact command and environment needed to run to reproduce the results. See the NeurIPS code and data submission guidelines (https://nips.cc/public/guides/CodeSubmissionPolicy) for more details.
- The authors should provide instructions on data access and preparation, including how to access the raw data, preprocessed data, intermediate data, and generated data, etc.
- The authors should provide scripts to reproduce all experimental results for the new proposed method and baselines. If only a subset of experiments are reproducible, they should state which ones are omitted from the script and why.
- At submission time, to preserve anonymity, the authors should release anonymized versions (if applicable).
- Providing as much information as possible in supplemental material (appended to the paper) is recommended, but including URLs to data and code is permitted.

6. **Experimental setting/details**

Question: Does the paper specify all the training and test details (e.g., data splits, hyperparameters, how they were chosen, type of optimizer, etc.) necessary to understand the results?

Answer: [Yes]

Justification: We have specifies all the training details in **Appendix A, B, C, D, E**.

Guidelines:

- The answer NA means that the paper does not include experiments.
- The experimental setting should be presented in the core of the paper to a level of detail that is necessary to appreciate the results and make sense of them.
- The full details can be provided either with the code, in appendix, or as supplemental material.

7. **Experiment statistical significance**

Question: Does the paper report error bars suitably and correctly defined or other appropriate information about the statistical significance of the experiments?

Answer: [No]

Justification: For FS-UCDR, following prior work, all results are obtained with the random seed fixed at 0. For few-shot classification, results are averaged over three independent runs with different random seeds.

Guidelines:

- The answer NA means that the paper does not include experiments.
- The authors should answer "Yes" if the results are accompanied by error bars, confidence intervals, or statistical significance tests, at least for the experiments that support the main claims of the paper.
- The factors of variability that the error bars are capturing should be clearly stated (for example, train/test split, initialization, random drawing of some parameter, or overall run with given experimental conditions).

- The method for calculating the error bars should be explained (closed form formula, call to a library function, bootstrap, etc.)
- The assumptions made should be given (e.g., Normally distributed errors).
- It should be clear whether the error bar is the standard deviation or the standard error of the mean.
- It is OK to report 1-sigma error bars, but one should state it. The authors should preferably report a 2-sigma error bar than state that they have a 96% CI, if the hypothesis of Normality of errors is not verified.
- For asymmetric distributions, the authors should be careful not to show in tables or figures symmetric error bars that would yield results that are out of range (e.g. negative error rates).
- If error bars are reported in tables or plots, The authors should explain in the text how they were calculated and reference the corresponding figures or tables in the text.

8. **Experiments compute resources**

   Question: For each experiment, does the paper provide sufficient information on the computer resources (type of compute workers, memory, time of execution) needed to reproduce the experiments?

   Answer: [Yes]

   Justification: As detailed in **Appendix C**, a single 24GB GPU is sufficient to reproduce all experiments.

   Guidelines:

   - The answer NA means that the paper does not include experiments.
   - The paper should indicate the type of compute workers CPU or GPU, internal cluster, or cloud provider, including relevant memory and storage.
   - The paper should provide the amount of compute required for each of the individual experimental runs as well as estimate the total compute.
   - The paper should disclose whether the full research project required more compute than the experiments reported in the paper (e.g., preliminary or failed experiments that didn't make it into the paper).

9. **Code of ethics**

   Question: Does the research conducted in the paper conform, in every respect, with the NeurIPS Code of Ethics https://neurips.cc/public/EthicsGuidelines?

   Answer: [Yes]

   Justification: We strictly follow the EthicsGuidelines.

   Guidelines:

   - The answer NA means that the authors have not reviewed the NeurIPS Code of Ethics.
   - If the authors answer No, they should explain the special circumstances that require a deviation from the Code of Ethics.
   - The authors should make sure to preserve anonymity (e.g., if there is a special consideration due to laws or regulations in their jurisdiction).

10. **Broader impacts**

    Question: Does the paper discuss both potential positive societal impacts and negative societal impacts of the work performed?

    Answer: [NA]

    Justification: NA.

    Guidelines:

    - The answer NA means that there is no societal impact of the work performed.
    - If the authors answer NA or No, they should explain why their work has no societal impact or why the paper does not address societal impact.

- Examples of negative societal impacts include potential malicious or unintended uses (e.g., disinformation, generating fake profiles, surveillance), fairness considerations (e.g., deployment of technologies that could make decisions that unfairly impact specific groups), privacy considerations, and security considerations.
- The conference expects that many papers will be foundational research and not tied to particular applications, let alone deployments. However, if there is a direct path to any negative applications, the authors should point it out. For example, it is legitimate to point out that an improvement in the quality of generative models could be used to generate deepfakes for disinformation. On the other hand, it is not needed to point out that a generic algorithm for optimizing neural networks could enable people to train models that generate Deepfakes faster.
- The authors should consider possible harms that could arise when the technology is being used as intended and functioning correctly, harms that could arise when the technology is being used as intended but gives incorrect results, and harms following from (intentional or unintentional) misuse of the technology.
- If there are negative societal impacts, the authors could also discuss possible mitigation strategies (e.g., gated release of models, providing defenses in addition to attacks, mechanisms for monitoring misuse, mechanisms to monitor how a system learns from feedback over time, improving the efficiency and accessibility of ML).

11. **Safeguards**

    Question: Does the paper describe safeguards that have been put in place for responsible release of data or models that have a high risk for misuse (e.g., pretrained language models, image generators, or scraped datasets)?

    Answer: [NA]

    Justification: This paper has no such tricks.

    Guidelines:

    - The answer NA means that the paper poses no such risks.
    - Released models that have a high risk for misuse or dual-use should be released with necessary safeguards to allow for controlled use of the model, for example by requiring that users adhere to usage guidelines or restrictions to access the model or implementing safety filters.
    - Datasets that have been scraped from the Internet could pose safety risks. The authors should describe how they avoided releasing unsafe images.
    - We recognize that providing effective safeguards is challenging, and many papers do not require this, but we encourage authors to take this into account and make a best faith effort.

12. **Licenses for existing assets**

    Question: Are the creators or original owners of assets (e.g., code, data, models), used in the paper, properly credited and are the license and terms of use explicitly mentioned and properly respected?

    Answer: [Yes]

    Justification: We have cited the original paper.

    Guidelines:

    - The answer NA means that the paper does not use existing assets.
    - The authors should cite the original paper that produced the code package or dataset.
    - The authors should state which version of the asset is used and, if possible, include a URL.
    - The name of the license (e.g., CC-BY 4.0) should be included for each asset.
    - For scraped data from a particular source (e.g., website), the copyright and terms of service of that source should be provided.
    - If assets are released, the license, copyright information, and terms of use in the package should be provided. For popular datasets, `paperswithcode.com/datasets` has curated licenses for some datasets. Their licensing guide can help determine the license of a dataset.

- For existing datasets that are re-packaged, both the original license and the license of the derived asset (if it has changed) should be provided.
- If this information is not available online, the authors are encouraged to reach out to the asset's creators.

13. **New assets**

    Question: Are new assets introduced in the paper well documented and is the documentation provided alongside the assets?

    Answer: [NA]

    Justification: The paper does not release new assets.

    Guidelines:

    - The answer NA means that the paper does not release new assets.
    - Researchers should communicate the details of the dataset/code/model as part of their submissions via structured templates. This includes details about training, license, limitations, etc.
    - The paper should discuss whether and how consent was obtained from people whose asset is used.
    - At submission time, remember to anonymize your assets (if applicable). You can either create an anonymized URL or include an anonymized zip file.

14. **Crowdsourcing and research with human subjects**

    Question: For crowdsourcing experiments and research with human subjects, does the paper include the full text of instructions given to participants and screenshots, if applicable, as well as details about compensation (if any)?

    Answer: [NA]

    Justification: This paper does not involve crowdsourcing nor research with human subjects.

    Guidelines:

    - The answer NA means that the paper does not involve crowdsourcing nor research with human subjects.
    - Including this information in the supplemental material is fine, but if the main contribution of the paper involves human subjects, then as much detail as possible should be included in the main paper.
    - According to the NeurIPS Code of Ethics, workers involved in data collection, curation, or other labor should be paid at least the minimum wage in the country of the data collector.

15. **Institutional review board (IRB) approvals or equivalent for research with human subjects**

    Question: Does the paper describe potential risks incurred by study participants, whether such risks were disclosed to the subjects, and whether Institutional Review Board (IRB) approvals (or an equivalent approval/review based on the requirements of your country or institution) were obtained?

    Answer: [NA]

    Justification: This paper does not involve crowdsourcing nor research with human subjects.

    Guidelines:

    - The answer NA means that the paper does not involve crowdsourcing nor research with human subjects.
    - Depending on the country in which research is conducted, IRB approval (or equivalent) may be required for any human subjects research. If you obtained IRB approval, you should clearly state this in the paper.
    - We recognize that the procedures for this may vary significantly between institutions and locations, and we expect authors to adhere to the NeurIPS Code of Ethics and the guidelines for their institution.
    - For initial submissions, do not include any information that would break anonymity (if applicable), such as the institution conducting the review.

16. **Declaration of LLM usage**

Question: Does the paper describe the usage of LLMs if it is an important, original, or non-standard component of the core methods in this research? Note that if the LLM is used only for writing, editing, or formatting purposes and does not impact the core methodology, scientific rigorousness, or originality of the research, declaration is not required.

Answer: [NA]

Justification: The core method development in this research does not involve LLMs as any important, original, or non-standard components

Guidelines:

- The answer NA means that the core method development in this research does not involve LLMs as any important, original, or non-standard components.
- Please refer to our LLM policy (https://neurips.cc/Conferences/2025/LLM) for what should or should not be described.

Summary of the Appendix

In the appendix of this paper, we provide further details:

- Elaboration on the used datasets (Appendix A).
- Explanation on the used metrics (Appendix B).
- Explanation on the implementation details (Appendix C).
- Elaboration on the used loss functions (Appendix D).
- Elaboration on the computational cost (Appendix E).
- Elaboration on the implementations for baseline methods (Appendix F).
- Additional design choices and details (Appendix G).
- Additional visualization results (Appendix H).
- Detailed experiment results with other shots under FS-UCDR (Appendix I).

A Datasets

A.1 Datasets for FS-UCDR and Its Variants

We conduct experiments on three datasets: DomainNet [38], Sketchy [41, 32], and TU-Berlin [12, 53]. **DomainNet** is utilized for UCDR and U^{D}CDR evaluations, comprising 596,006 images across six domains: *Real*, *Sketch*, *Quickdraw*, *Infograph*, *Clipart*, and *Painting*. Following the leave-one-out protocol from ProS, five domains serve as sources, while the remaining one acts as the unseen query domain. The $\mathrm{MixedGallery}$ is created by combining the $\mathrm{UnseenGallery}$ with 8% of samples from each seen class in the *Real* domain. For U^{D}CDR evaluation, we select 45 training classes and use 25% of the samples from each class for both the query domain (10% for *Quickdraw*) and the *Real* domain. The **Sketchy** and **TU-Berlin** datasets are employed for U^{C}CDR evaluation, each containing two domains: *Real* and *Sketch*. Detailed statistics of the datasets are summarized in **Tab. 8**.

Table 8: Statistics of the utilized datasets for FS-UCDR and its variants. The average shots denotes the average number of images per class in each domain.

Dataset	Images	Domains	Classes	Train Classes	Val Classes	Test Classes	Average Shots
DomainNet	596006	6	345	245	55	45	287.9
Sketchy	148473	2	125	93	11	21	593.9
TU-Berlin	224489	2	250	200	20	30	449.0

A.2 Datasets for Few-Shot Classification.

Base-to-Novel Generalization: In this evaluation, the dataset's categories are partitioned equally into base and novel classes. The model is trained solely on the base classes and evaluated on both base and novel classes. This setup enables us to assess the model's transfer learning performance on seen categories. We conduct this evaluation across 11 diverse image classification datasets: ImageNet [9], Caltech101 [14], OxfordPets [36], StanfordCars [29], Flowers102 [34], Food101 [2], FGVCAircraft [33], SUN397 [48], UCF101 [35], DTD [8], and EuroSAT [17].

Cross-Dataset Evaluation: This evaluation tests how well the model works on new datasets it has never seen before. Like CoCoOp [56], we first train the model on all 1000 ImageNet classes using only a few examples per class. Then, we directly apply the trained model to other datasets to see if it can generalize across datasets. The target datasets used are the ten remaining datasets in the base-to-novel generalization experiment.

Domain Generalization: In this setup, similar to cross-dataset evaluation, we also use ImageNet for training, and evaluate on four domain-shifted variants—ImageNetV2 [40], ImageNet-Sketch [46], ImageNet-A [19], and ImageNet-R [18]—each presenting a distinct type of domain variation.

Detailed statistics of the datasets are summarized in **Tab. 9**.

Table 9: Statistics of the utilized datasets for few shot classification. * denotes the number of images.

Dataset	Classes	Train*	Val*	Test*	Prompt
ImageNet	1000	1.28M	∼	50000	"a photo of a <category>."
Caltech101	100	4128	1649	2465	"a drawing of a <category>."
OxfordPets	37	2944	736	3669	"an awesome animal pet photo of a <category>."
StanfordCars	196	6509	1635	8041	"a photo of my <category>."
Flowers102	102	4093	1633	2463	"a flower photo of a <category>."
Food101	101	50500	20200	30300	"a food photo of a <category>."
FGVCAircraft	100	3334	3333	3333	"a brand aircraft a <category>."
SUN397	397	15880	3970	19850	"a scene photo of a <category>."
DTD	47	2820	1128	1692	"a beautiful texture drawing a <category>."
EuroSAT	10	13500	5400	8100	"a photo of a <category>, a type of centered satellite."
UCF101	101	7639	1898	3783	"a photo of a <category>, a type of action."
ImageNetV2	1,000	∼	∼	10,000	"a photo of a <category>."
ImageNet-Sketch	1,000	∼	∼	50,889	"a sketch photo of a <category>."
ImageNet-A	200	∼	∼	7,500	"a poor photo of a <category>."
ImageNet-R	200	∼	∼	30,000	"a sketch photo of a <category>."

A.3 Practicality of FS-UCDR

1. Data collection is hard. UCDR relies on DomainNet [38] as its benchmark dataset, where each domain contains an average of 287.9 samples per class, resulting in approximately 1,400 samples per class across five diverse domains. For comparison, ImageNet—commonly used in few-shot learning—contains roughly 1,200 to 1,300 samples per class. Although the per-class sample sizes are similar, collecting DomainNet-style multi-domain data is significantly more challenging than collecting single-domain (real-world) images like those in ImageNet. While automated data collection may be feasible for domains such as Real, it is much harder for others like Clipart or Sketch. Therefore, developing and studying the few-shot UCDR setting is both meaningful and necessary, as it reduces data requirements while maintaining the core challenge of cross-domain generalization.

2. More data does not help. Since UCDR involves unseen domains and classes during testing, the inherent domain and semantic shifts between training and testing phases may increase the risk of overfitting for PEFT methods when more training data is used. This phenomenon is supported by empirical evidence: as shown in the **Tab. 10**, the average mAP for 2-shot and full-shot settings is 62.05% and 61.95%, respectively. This indicates that increasing the number of training samples does not necessarily lead to better performance, further highlighting the relevance of the FS-UCDR setting.

Table 10: The average performance of MAIL across five query domains under varying shot settings in the FS-UCDR task. Bold values denote the best performance. Results from 2-shot UCDR experiments are highlighted with a light purple background, while those from full-shot UCDR experiments are highlighted with a light grey background.

Shot	**UnseenGallery**		**MixedGallery**	
	mAP_{200}	Prec_{200}	mAP_{all}	Prec_{100}
1	60.40	56.12	54.70	50.87
2	62.05	58.31	56.05	52.80
4	63.64	59.94	57.71	54.63
8	63.75	60.19	57.72	54.62
16	**63.77**	**60.42**	**57.75**	**54.66**
32	63.52	60.13	57.52	54.13
64	63.21	59.82	57.31	53.95
128	62.79	59.42	57.01	53.54
FULL (287.9)	61.95	58.12	56.60	52.96

B Evaluation Metrics

For FS-UCDR, FS-U^{D}CDR, and FS-U^{C}CDR, following prior work ProS [13], we adopt the same evaluation metrics. For the Sketchy and DomainNet datasets, **precision** (Prec_{200}) and **mean Average Precision** (mAP_{200}) are calculated based on the top-200 retrieved results. For the TU-Berlin dataset, we use Prec_{100} and mAP_{all} as the evaluation metrics. As for the few-shot classification, the **classification accuracy** is adopted.

C Implementation Details.

C.1 Implementation Details for FS-UCDR and Its Variants

When CLIP [39] is applied in UCDR tasks, the ViT-B/32 [11] backbone is most commonly used [13]. We follow this convention and utilize a pre-trained ViT-B/32 [11] CLIP model with $d_t = 512$ and $d_v = 768$, the rank (r) of the bridge function in MAIL, is set to 8. The text prompt is fixed as "`a photo of a <category>`".

For DomainNet, training is limited to 1 epoch, whereas Sketchy and TU-Berlin are trained for 20 epochs, with early stopping applied after 2 epochs. Given the diverse source domains in FS-UCDR, we organize each batch as $B = N_s \times C_b \times k_b$, where N_s represents the number of source domains, $C_b = 3$ denotes the number of classes sampled from each domain (we sample different classes for each domain), and $k_b = 4$ denotes the number of images for each class from each source domain within the batch. Note that if $k_b > k$, repeated images will appear in the batch, with k denotes the shot number.

The optimization is performed using the Adam optimizer with a learning rate of $2e-4$ and a cosine decay schedule. All experiments are conducted on a single NVIDIA RTX 4090 GPU with mixed-precision training to accelerate computation. To ensure reproducibility, we follow the setting in ProS [13] and fix the random seed to 0. A 2-shot training strategy is employed, where two samples per class per domain are randomly selected. For the used loss functions and the results with other shot configurations, one can refer to **Appendix D** and **Appendix I**.

C.2 Implementation Details for Few-Shot Classification

We follow prior studies [57, 56, 24, 49], the ViT-B/16 [11] variant of the CLIP model serves as the visual backbone for all experimental setups, with $d_t = 512$ and $d_v = 768$, the rank (r) of the bridge function in MAIL, is set to 32. Hand-crafted text prompts from prior methods [39, 57, 55] are utilized and described in detail in **Tab. 9**. A 16-shot training strategy is employed, where 16 samples per class are randomly selected. The average accuracy is reported over three independent runs with random seeds set to 0, 1, and 2. All experiments are conducted on a single NVIDIA RTX 4090 GPU.

For **base-to-novel evaluation**, we adopt a batch size of 64 for the larger datasets (ImageNet and SUN397) and 4 for all others. Training is performed for 5 epochs on ImageNet and 10 epochs on the remaining datasets. We employ the AdamW optimizer for all experiments, except on EuroSAT, where the SGD optimizer yields better performance. The initial learning rate is set to 5.0×10^{-6} for Food101, 2.5×10^{-5} for DTD, and 1.5×10^{-5} for the other datasets. The rank (r) of the bridge is set to 12 for DTD and 32 for the remaining datasets.

For **cross-dataset evaluation and domain generalization tasks,** we train the model on ImageNet for 2 epochs. Due to GPU memory constraints—mainly caused by the full 1000-class setting, which is twice the size of the base-to-novel evaluation (500 classes)—we reduce the batch size from 64 to 32 and use half-precision training (fp16). The initial learning rate is set to $2.5e-5$.

D Loss Function

Given the diverse source domains in FS-UCDR, we organize each batch as $B = N_s \times C_b \times k_b$, where N_s represents the number of source domains, $C_b = 3$ denotes the number of classes sampled from each domain (we sample different classes for each domain), and $k_b = 4$ denotes the number of images for each class from each source domain within the batch. Note that if $k_b > k$, repeated images will appear in the batch, with k denotes the shot number. We utilize two loss functions: the image-text matching loss and the triplet-hard loss [20]. The image-text matching loss is defined as a

cross-entropy loss:

$$\mathcal{L}_{ce} = \frac{1}{B}\sum_{j=1}^{B} -y_j \log \frac{\exp(sim(\mathcal{T}(t_{y_j}), \mathcal{V}(I_j)))}{\sum_{i=1}^{C} \exp(sim(\mathcal{T}(t_i), \mathcal{V}(I_j)))}, \tag{9}$$

where I_j is the j-th image in the batch, and y_j is the corresponding label.

The triple-hard loss is formulate as:

$$\mathcal{L}_{tri\_hard} = \frac{1}{B}\sum_{i=1}^{P}\sum_{a=1}^{K}[\rho - \min_{p=1\ldots K} sim(\mathcal{V}(I_i^a), \mathcal{V}(I_i^p)) + \max_{\substack{j=1\ldots P \\ j\neq i \\ n=1\ldots K}} sim(\mathcal{V}(I_i^a), \mathcal{V}(I_j^n))]_+, \tag{10}$$

where $\rho = 0.5$ is the margin hyper-parameter, $P = C_b$ denotes the number of identities within the batch, and $K = N_S \times k_b$ is the total number of samples for each class across all the source domains. $[\cdot]_+$ denotes the $max(0, \cdot)$ function, $sim(\cdot, \cdot)$ represents cosine similarity, and I_i^a identifies the anchor image, specifically the a-th image from the i-th class within the batch. Additionally, I_i^p refers to the positive sample, while I_j^n corresponds to the negative sample.

In terms of the **few-classification task**, we only utilize the cross-entropy loss.

E Computational Cost

To validate the efficiency of our method, we present the computational costs of MAIL in **Fig. 7**. Both the training and inference stages utilize a batch size of 60. Compared to MMA and MaPLe, while MAIL incurs higher computational costs during training—including memory usage and training time—it reduces test time, inference memory, and GFLOPs. These results highlight the superior efficiency of MAIL during inference. Please note these results are obtained under FS-UCDR's UnseenGallery scenario, where *Sketch* domain is used as the query domain.

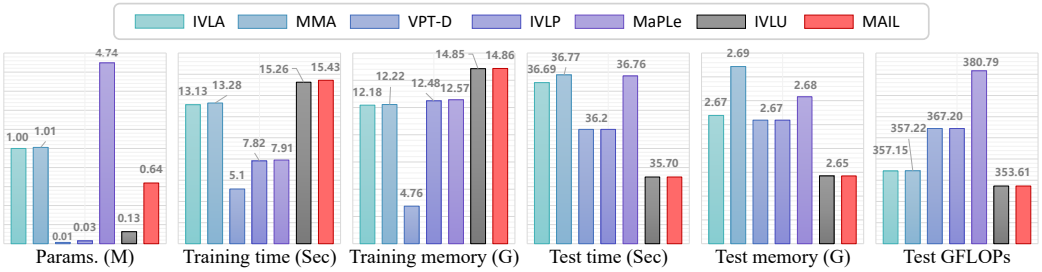

Figure 7: Computational costs of various tuning methods, presented from left to right: the number of trainable parameters, training time (per epoch), training memory usage, test time, test memory usage, and test GFLOPs.

F Implementation of Baseline Methods under FS-UCDR and Its Variants

We re-implement VPT-Deep [23], IVLP [24], MaPLe [24], MMA [49], AdaptFormer [6] and IVLA [49] based on the released code. Specifically, the configurations for VPT-Deep, IVLP, and MaPLe are mainly taken directly from the MaPLe paper. However, while the original prompt depth for MaPLe ranges from 1 to 9, we find that a depth of 1 to 12 performs significantly better for our task. The configurations for VPT-Deep, IVLP and MaPLe, are as follows:

Table 11: The used configurations for VPT-D, IVLP, and MaPLe. PL denotes the prompt length.

METHOD	PL-VISUAL	PL-TEXTUAL	PROMPT DEPTH	LEARNING RATE
VPT-D	4	0	1-12	0.0002
IVLP	2	2	1-12	0.0002
MAPLE	2	2	1-12	0.0002

For AdaptFormer, IVLA and MMA, we adopt the configurations outlined in the MMA paper, with one exception regarding the depth parameter. While the MMA paper sets the depth to 9-12 for cross-dataset evaluation, we find that a depth of 1-12 performs better under FS-UCDR. The configurations for AdaptFormer, IVLA and MMA, are as follows:

Table 12: The used configurations for IVLA and MMA.

METHOD	ADAPTER RANK	ADAPTER DEPTH	LEARNING RATE
ADAPTFORMER	32	1-12	0.0015
IVLA	32	1-12	0.0015
MMA	32	1-12	0.0015

For LoRA[22], we adopt the implementation from CLIP-LoRA [22], with an initial learning rate of 0.0005, and the rank of the low-rank matrices, is set to 6 after hyper-parameter tuning. For BitFit [52], we fine-tune **all** bias terms in the CLIP backbone, using an initial learning rate of 0.0002. All other configurations, including batch size and loss functions, are kept identical to those used in our MAIL.

Note that LoRA performs poorly from the main body. To further investigate this issue, we conduct additional experiments under the FS UCDR setting, where we replace CLIP with our trained MAIL as the backbone for LoRA. The results are presented in **Tab. 13**, showing that LoRA remains inferior to MAIL and even degrades its performance. We believe this is an interesting open question for future research—why LoRA, despite its effectiveness in many scenarios, performs poorly in this context.

Table 13: FS-UCDR (2-shot) evaluation results (%) on DomainNet. * denotes the results are obtained using the full training data, i.e., the UCDR results. † denotes that the results are obtained when our MAIL is used as backbone.

Methods	*Sketch*				*Quickdraw*				*Painting*			
	UnseenGallery		**MixedGallery**		**UnseenGallery**		**MixedGallery**		**UnseenGallery**		**MixedGallery**	
	mAP_{200}	$Prec_{200}$	mAP_{200}	$Prec_{200}$	mAP_{200}	$Prec_{200}$	mAP_{200}	$Prec_{200}$	mAP_{200}	$Prec_{200}$	mAP_{200}	$Prec_{200}$
ProS* [CVPR'24]	64.67	60.01	58.43	54.63	28.42	25.44	23.18	21.27	75.16	69.55	71.20	66.12
CLIP [ICML'21]	42.20	35.28	36.62	29.79	7.44	5.61	6.00	3.17	61.68	55.07	56.53	50.14
LoRA [ICLR'22]	54.85	49.23	48.71	43.33	22.16	18.10	17.73	14.21	71.46	65.10	66.81	60.81
LoRA† [ICLR'22]	64.74	60.41	56.82	52.90	27.98	25.39	20.40	18.63	74.95	68.37	69.44	64.33
MAIL [Ours]	**65.76**	**61.57**	**59.05**	**55.25**	29.41	26.95	22.83	21.26	**76.05**	**70.85**	**71.12**	**66.44**

Methods	*Infograph*				*Clipart*				*Average*			
	UnseenGallery		**MixedGallery**		**UnseenGallery**		**MixedGallery**		**UnseenGallery**		**MixedGallery**	
	mAP_{200}	$Prec_{200}$	mAP_{200}	$Prec_{200}$	mAP_{200}	$Prec_{200}$	mAP_{200}	$Prec_{200}$	mAP_{200}	$Prec_{200}$	mAP_{200}	$Prec_{200}$
ProS* [CVPR'24]	57.98	54.42	52.19	49.56	76.48	71.86	72.28	68.15	60.52	56.26	55.46	51.95
CLIP [ICML'21]	50.08	44.74	43.75	38.91	60.37	51.30	56.08	46.91	44.35	38.40	39.80	33.78
LoRA [ICLR'22]	58.01	53.84	51.86	48.20	70.52	64.11	66.00	59.63	55.40	50.08	50.22	45.24
LoRA† [ICLR'22]	58.96	55.04	52.30	50.26	77.12	72.56	72.02	67.25	60.75	56.35	54.20	50.67
MAIL [Ours]	**60.11**	**57.40**	**53.34**	**50.95**	**78.94**	**74.80**	**73.91**	**70.14**	**62.05**	**58.31**	**56.05**	**52.80**

G Additional Design Choices and Details

G.1 Linear Layer Bridge Function

The bridge function in our MAIL is a bottleneck structure, although it could be implemented as a simple linear layer. In our experiments, we find that the linear layer not only has significantly more trainable parameters but also performs worse than the bottleneck structure. The results are as follows:

Table 14: Ablation studies on linear layer bridge function. We present the average performance scores on DomainNet across five query domains under FS-UCDR.

Methods	**UnseenGallery**		**MixedGallery**		**Params.** (↓)
	mAP_{200}	$Prec_{200}$	mAP_{all}	$Prec_{100}$	
V → L (Linear Layer)	58.49	54.65	53.53	49.50	19657216
V ↔ L (Linear Layer)	61.32	57.46	55.39	52.04	39186944
V ← L (Linear Layer)	61.40	57.53	55.52	52.16	19657216
V ← L (Bottleneck)	**62.05**	**58.31**	**56.05**	**52.80**	**637400**

G.2 Initialization Method of the Bridge Function

Next, we exam the initialization method of the bridge function. As noted in the main body, W_{down} is initialized with random Gaussian values, while W_{up} is initialized to zeros, i.e., $W_{down} \sim \mathcal{N}(0, \sigma_t^2)$, with $\sigma_t = \frac{1}{\sqrt{d_t}}$, $W_{up} = 0$. Here we conduct more experiments about the initialization of the two matrices, the results, are as follows:

Table 15: Ablation studies on different initialization methods of W_{down} and W_{up}. Note that if W_{down} or W_{up} are initialized with Uniform values, then, $W_{down} \sim U(-\frac{\sqrt{12\sigma_t^2}}{2}, \frac{\sqrt{12\sigma_t^2}}{2})$ and $W_{up} \sim U(-\frac{\sqrt{12\sigma_v^2}}{2}, \frac{\sqrt{12\sigma_v^2}}{2})$, with $\sigma_v = \frac{1}{\sqrt{d_v}}$. Similarly, if W_{up} is initialized with Gaussian values, then, $W_{up} \sim \mathcal{N}(0, \sigma_v^2)$. We present the average performance scores for the UnseenGallery and MixedGallery scenarios on DomainNet across five query domains under FS-UCDR.

W_{down}	W_{up}	**UnseenGallery**		**MixedGallery**	
		mAP_{200}	Prec_{200}	mAP_{all}	Prec_{100}
0	Uniform	59.94	56.05	53.99	50.53
0	Gaussian	60.47	56.48	54.48	50.98
0	0	58.77	54.17	53.08	48.92
Uniform	Uniform	59.61	55.65	53.66	50.14
Uniform	0	62.01	58.16	55.83	52.59
Gaussian	Gaussian	59.89	55.88	53.95	50.43
Gaussian	0	**62.05**	**58.31**	**56.05**	**52.80**

From **Tab. 15**, we observe that the Gaussian distribution achieves slightly better performance compared with the uniform distribution. We encourage readers to explore additional distributions.

G.3 Should the Shifting Vectors in the Agent Layers Be Connected Across Modalities?

Note that we only apply the bridge function to the scaling vectors a across modalities. To address the question above, we conducted the following experiments, selectively adding or removing bridge functions from the shifting vectors b:

Table 16: Ablation studies on bridge function applied to the shifting vector b. We present the average performance scores on DomainNet across five query domains under FS-UCDR.

Methods	**UnseenGallery**		**MixedGallery**		**Params.** (↓)
	mAP_{200}	Prec_{200}	mAP_{all}	Prec_{100}	
w Bridge Function	**62.26**	**58.50**	**56.23**	**53.01**	1147392
w/o Bridge Function	62.05	58.31	56.05	52.80	**637400**

As we can see from **Tab. 16**, the introduction of the bridge function to the shifting vectors b does improve performance; however, this improvement is limited. Furthermore, it results in doubling the number of trainable parameters, which creates a poor trade-off. Therefore, we propose to remove the bridge function from the shifting vectors.

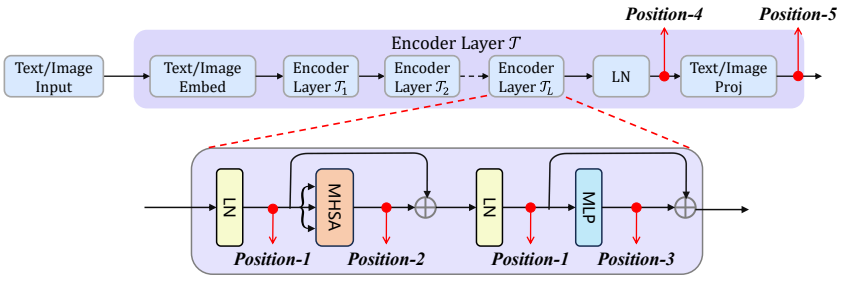

Figure 8: The five types of insertion locations.

G.4 Discussion About the Insert Locations.

We have utilized about five types of insert locations (**Fig. 8**):

- ***Position-1&2&3***: In the transformer block, insert the agent layer after each LayerNorm (LN) & MHSA & MLP layer.

- ***Position-4&5***: Out of the transformer block, insert the agent layer after the last LN & projection layer.

We select these five positions for ease of implementation. For clarity, we illustrate only positions 1, 2, and 3. The pseudocode for the Transformer block is presented in **Alg. 1**. As shown, incorporating our modifications requires adding just four lines of code, as depicted in **Alg. 2**, ensuring minimal code changes. Additionally, the definition of MAIL is located outside the transformer block (**Alg. 3**).

Algorithm 1 Pseudocode for the Transformer block within CLIP, presented in a PyTorch-like style.

```
# x:       features from the last transformer block
# y:       features to the next transformer block
# LN:      layer normalization
# MHSA:    multi-head self-attention
# MLP:     multilayer perceptron
# flag:    indicates whether the current block from the image encoder or the text encoder.

x = LN(x) # We can insert MAIL here
# 1. x = MAIL(x, flag)
mhsa = MHSA(x) # We can insert MAIL here
# 2. mhsa = MAIL(mhsa, flag)
x = x + mhsa
x = LN(x)# We can insert MAIL here
# 3. x = MAIL(x, flag)
mlp = MLP(x)# We can insert MAIL here
# 4. mlp = MAIL(mlp, flag)
y = x + mlp
```

Algorithm 2 Pseudocode for the Transformer block with MAIL integration within CLIP, presented in a PyTorch-like style.

```
# flag:    indicates whether the current block from the image encoder or the text encoder.
# MAILs:   a list containg 4 MAIL blocks

x = LN(x)
x = MAILs[0](x, flag) # position-1
mhsa = MHSA(x)
mhsa = MAILs[1](mhsa, flag) # position-2
x = x + mhsa
x = LN(x)
x = MAILs[2](x, flag) # position-1
mlp = MLP(x)
mlp = MAILs[3](mlp, flag) # position-3
y = x + mlp
```

Algorithm 3 Pseudocode of MAIL in a PyTorch-like style.

```
# x:              input feature
# y:              output feature
# flag:           indicates whether  x  from the image encoder or the text encoder.
# imageAgent:     the agent layer for the image encoder
# textAgent:      the agent layer for the text encoder
# W:              bridge function

if flag==''text'':
   y = x * textAgent.a + textAgent.b
else:
   a = imageAgent.a + textAgent.a @ W.down @ W.up
   y = x * a + visionAgent.b
```

H Visualization

H.1 T-SNE Visualization

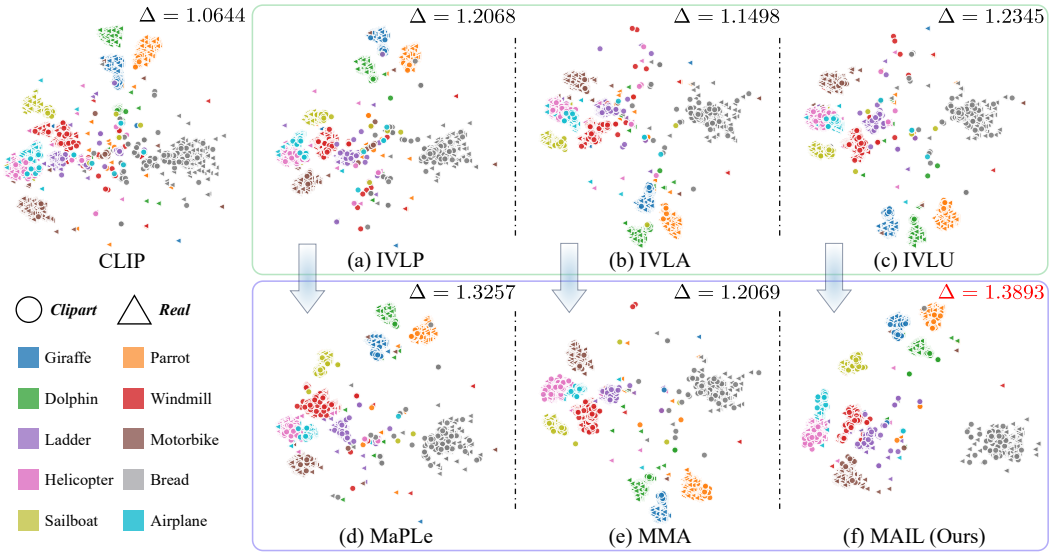

Figure 9: The t-SNE visualization for 10 randomly selected unseen classes of *Clipart* (query) domains and *Real* (gallery) domain. Different colors represent different classes, while △ and ◯ represent samples from *Real* and *Clipart* domains, respectively. we also evaluate the inter-class distinctiveness and intra-class compactness of feature space by the metric $\Delta = \frac{\text{mean } \mathcal{D}_{inter}}{\text{mean } \mathcal{D}_{intra}}$ (higher is better).

As shown in **Fig. 9**, we visualize the image features extracted from frozen CLIP, IVLP, IVLA, IVLU, MaPLe, MMA, and our MAIL method for 10 randomly selected unseen classes from the *Real* and unseen *Clipart* domains using t-SNE [44]. We also evaluate the inter-class distinctiveness and intra-class compactness of the feature space using the metric

$$\Delta = \frac{\text{mean } \mathcal{D}_{inter}}{\text{mean } \mathcal{D}_{intra}}, \tag{11}$$

where $\mathcal{D}_{inter}$ is a set that measures distances between all centers testing classes:

$$\mathcal{D}_{inter} = \{d(c^i, c^j) | i = 1, 2, ..., C_{test}, j = i + 1, ..., C_{test}\}. \tag{12}$$

Here, C_{test} denotes the number of classes during the test, $c^i = \frac{1}{n_i} \sum_{k=1}^{n_i} b_k^i$ is the centroid of the i-th class, with n_i being the number of samples in the i-th class, b_k^i denoting the sample, and $d(\cdot, \cdot)$ representing the Euclidean distance.

Similarly, $\mathcal{D}_{intra}$ measures the distances among samples of the same class relative to their corresponding centroid:

$$\mathcal{D}_{intra} = \{d^i | i = 1, 2, ..., C_{test}\}, \tag{13}$$

where $d^i = \frac{1}{n_i} \sum_{k=1}^{n_i} d(b_k^i, c^i)$ indicates the compactness of the i-th class.

From **Fig. 9**, we can observe that modality-coupled methods better align feature representations of the same classes between the two domains and exhibit greater separation between different classes compared to modality-independent methods. Furthermore, our MAIL method achieves the best results in both the visualization and numeric metric evaluations.

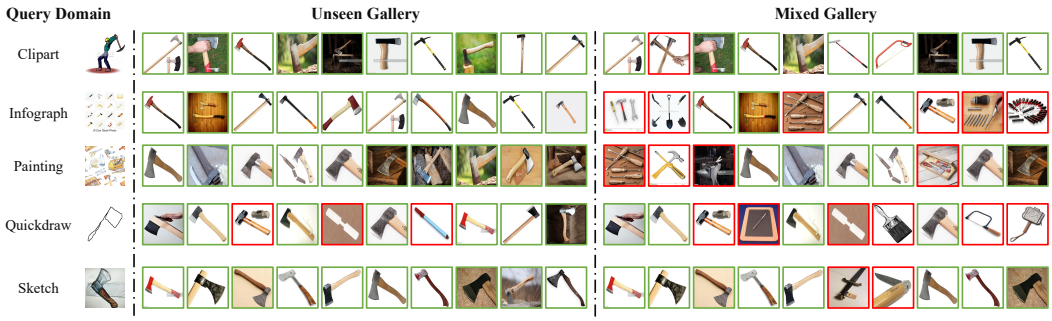

Figure 10: Retrieval results with query classes *axe*. Please zoom in for a better resolution.

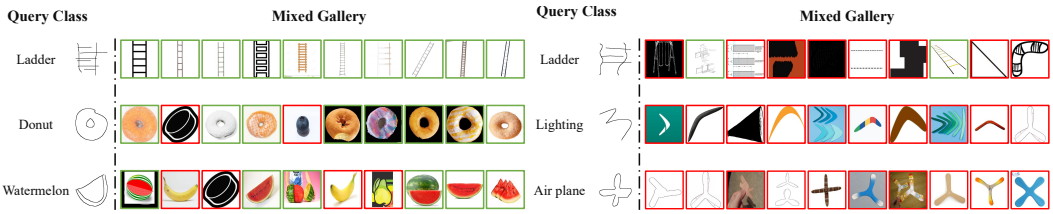

Figure 11: Retrieval results in query domain *Quickdraw*. Please zoom in for a better resolution.

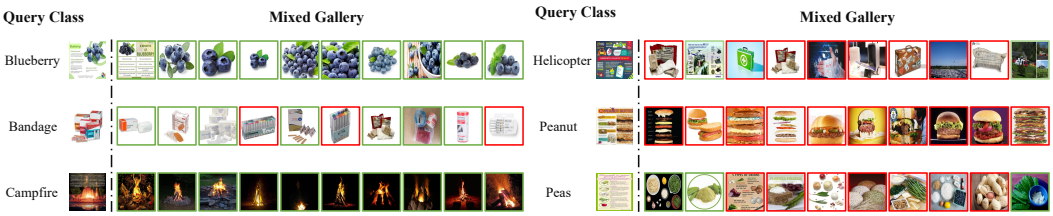

Figure 12: Retrieval results in query domain *Infograph*. Please zoom in for a better resolution.

H.2 Top-10 Retrieved Results

To further evaluate the effectiveness of MAIL, we visualize several retrieval results. **Fig. 10** presents the top-10 retrieved candidates for the category "axe" using query images from different domains, while **Fig. 11** and **Fig. 12** display the top-10 retrieval results for queries originating from the *Quickdraw* domain.

These visualizations demonstrate that while MAIL achieves strong retrieval performance overall, its effectiveness is occasionally hindered by *query ambiguity*. This issue arises primarily from two factors: (1) **Lack of detail**: Queries from the *Quickdraw* domain often contain simplistic or abstract sketches, making them inherently ambiguous and prone to misinterpretation. (2) **Object clutter**: Queries from the *Infograph* domain frequently depict multiple objects within a single image, introducing uncertainty regarding the intended retrieval target. These challenges highlight potential areas for further refinement in handling ambiguous queries across diverse domains.

I Evaluation Results with Other Shots

While the 2-shot results are presented in the main body, we provide additional results for other shot settings in this section: 1-shot, 3-shot, 4-shot, and 8-shot. As observed in the tables below, the performance of all methods improves with an increased number of shots. Notably, our method consistently outperforms its competitors. Furthermore, it is important to emphasize that nearly all methods surpass ProS with a sufficient number of shots (significantly fewer than full shots).

I.1 1-Shot Results

Table 17: 1-shot UCDR evaluation results (%) on DomainNet.

Methods	*Sketch*				*Quickdraw*				*Painting*			
	Unseen Gallery		**Mixed Gallery**		**Unseen Gallery**		**Mixed Gallery**		**Unseen Gallery**		**Mixed Gallery**	
	mAP_{200}	$Prec_{200}$	mAP_{200}	$Prec_{200}$	mAP_{200}	$Prec_{200}$	mAP_{200}	$Prec_{200}$	mAP_{200}	$Prec_{200}$	mAP_{200}	$Prec_{200}$
ProS*	64.67	60.01	58.43	54.63	28.42	25.44	23.18	21.27	75.16	69.55	71.20	66.12
ZS CLIP	42.20	35.28	36.62	29.79	7.44	5.61	6.00	3.17	61.68	55.07	56.53	50.14
VPT-D	55.16	49.98	48.48	43.71	21.22	19.20	15.94	14.36	69.71	63.05	64.76	58.46
AdaptFormer	49.73	43.15	43.55	37.33	11.35	9.29	8.63	5.88	65.00	57.75	59.86	53.04
IVLP	51.41	46.31	45.18	40.19	13.10	11.95	9.65	8.08	68.42	62.08	63.32	57.38
IVLA	51.23	44.82	44.94	38.93	12.72	10.58	9.69	6.90	65.75	58.61	60.63	53.92
MaPLe	60.31	55.51	53.59	49.20	25.91	23.52	20.06	18.29	74.03	68.18	69.27	63.74
MMA	53.15	46.85	46.15	40.83	15.29	12.68	11.66	8.75	66.73	59.81	61.63	55.15
MAIL	**63.25**	**58.59**	**56.67**	**52.43**	**27.56**	**24.82**	**21.73**	**19.78**	**74.53**	**68.78**	**69.75**	**64.41**

Methods	*Infograph*				*Clipart*				*Average*			
	Unseen Gallery		**Mixed Gallery**		**Unseen Gallery**		**Mixed Gallery**		**Unseen Gallery**		**Mixed Gallery**	
	mAP_{200}	$Prec_{200}$	mAP_{200}	$Prec_{200}$	mAP_{200}	$Prec_{200}$	mAP_{200}	$Prec_{200}$	mAP_{200}	$Prec_{200}$	mAP_{200}	$Prec_{200}$
ProS*	57.98	54.42	52.19	49.56	76.48	71.86	72.28	68.15	60.52	56.26	55.46	51.95
ZS CLIP	50.08	44.74	43.75	38.91	60.37	51.30	56.08	46.91	44.35	38.40	39.80	33.78
VPT-D	53.82	49.27	47.11	43.17	69.30	63.65	64.55	58.95	53.84	49.03	48.17	43.73
AdaptFormer	55.05	49.40	49.34	44.23	65.51	57.30	61.09	52.89	49.33	43.38	44.94	38.67
IVLP	56.59	51.91	50.09	45.99	68.32	62.44	63.84	58.02	47.21	41.41	42.73	37.15
IVLA	55.66	50.16	49.92	44.94	65.73	56.42	62.34	54.42	50.22	44.12	45.50	39.82
MaPLe	**59.56**	56.02	**52.85**	49.63	75.67	70.64	70.83	65.92	59.09	54.77	53.32	49.35
MMA	56.62	51.37	50.72	45.98	67.95	60.25	63.47	55.82	51.94	46.19	46.73	41.31
MAIL	59.48	**56.29**	52.83	**49.99**	**77.19**	**72.13**	**72.53**	**67.72**	**60.40**	**56.12**	**54.70**	**50.87**

Table 18: 1-shot U^DCDR evaluation results (%) on DomainNet.

Methods	*Sketch*		*Quickdraw*		*Painting*		*Infograph*		*Clipart*		*Average*	
	mAP_{200}	$Prec_{200}$	mAP_{200}	$Prec_{200}$	mAP_{200}	$Prec_{200}$	mAP_{200}	$Prec_{200}$	mAP_{200}	$Prec_{200}$	mAP_{200}	$Prec_{200}$
ProS*	73.85	49.11	28.89	11.86	72.27	46.15	60.56	39.62	81.05	52.98	63.32	39.94
ZS CLIP	47.60	28.71	8.67	4.50	55.69	31.70	47.56	29.36	55.81	31.10	43.07	25.07
VPT-D	62.69	40.36	20.04	8.91	63.44	38.43	55.64	35.40	69.49	42.50	54.26	33.12
AdaptFormer	55.36	33.66	11.75	5.63	58.74	32.41	54.15	31.65	61.41	34.99	48.28	27.67
IVLP	59.60	38.37	15.97	7.73	63.40	37.86	57.27	35.49	67.76	40.84	52.80	32.05
IVLA	57.31	34.97	12.81	5.99	59.59	33.05	55.07	32.35	62.83	35.98	49.52	28.47
MaPLe	68.54	45.29	25.18	10.80	69.06	43.30	60.06	39.10	76.15	48.14	59.79	37.33
MMA	59.39	36.31	14.38	6.40	60.67	33.98	56.20	33.27	64.27	37.02	50.98	29.39
MAIL	**70.28**	**45.79**	**25.79**	**11.06**	**70.15**	**43.15**	**60.19**	**39.09**	**77.10**	**48.66**	**60.70**	**37.61**

Table 19: 1-shot U^CCDR evaluation results (%) on Sketchy and TU-Berlin.

Methods	**Sketchy**		**TU-Berlin**	
	mAP_{200}	$Prec_{200}$	mAP_{all}	$Prec_{100}$
ProS*	69.91	65.45	66.75	74.42
ZS CLIP	35.82	33.08	31.45	46.12
VPT-D	58.43	53.74	57.91	67.81
AdaptFormer	52.15	48.87	46.38	60.52
IVLP	51.98	47.76	53.33	65.16
IVLA	52.17	48.89	46.85	60.76
MaPLe	**65.95**	**61.51**	63.00	71.85
MMA	52.53	49.31	50.26	63.68
MAIL	65.70	61.24	**65.30**	**73.82**

I.2 3-Shot Results

Table 20: 3-shot UCDR evaluation results (%) on DomainNet.

Methods	*Sketch*				*Quickdraw*				*Painting*			
	Unseen Gallery		**Mixed Gallery**		**Unseen Gallery**		**Mixed Gallery**		**Unseen Gallery**		**Mixed Gallery**	
	mAP_{200}	$Prec_{200}$	mAP_{200}	$Prec_{200}$	mAP_{200}	$Prec_{200}$	mAP_{200}	$Prec_{200}$	mAP_{200}	$Prec_{200}$	mAP_{200}	$Prec_{200}$
ProS*	64.67	60.01	58.43	54.63	28.42	25.44	23.18	21.27	75.16	69.55	71.20	66.12
ZS CLIP	42.20	35.28	36.62	29.79	7.44	5.61	6.00	3.17	61.68	55.07	56.53	50.14
VPT-D	60.47	55.78	53.00	48.80	23.83	21.17	18.16	16.44	73.32	67.32	68.20	62.61
AdaptFormer	64.44	59.53	57.38	53.05	27.28	24.45	21.75	19.70	74.47	68.63	69.67	64.27
IVLP	59.66	55.05	52.37	48.30	22.53	20.13	16.77	15.27	72.64	66.89	67.50	62.16
IVLA	63.77	59.91	57.68	53.40	26.16	24.31	20.58	19.57	74.30	68.52	69.44	64.10
MaPLe	64.38	59.88	57.46	53.48	26.64	23.86	21.06	19.14	75.55	70.00	70.91	65.79
MMA	65.99	61.55	59.04	55.11	27.61	25.19	21.79	20.29	75.52	70.07	70.70	65.68
MAIL	**67.68**	**63.63**	**60.81**	**57.24**	**28.15**	**25.70**	**22.24**	**20.55**	**77.22**	**72.07**	**72.35**	**67.69**

Methods	*Infograph*				*Clipart*				*Average*			
	Unseen Gallery		**Mixed Gallery**		**Unseen Gallery**		**Mixed Gallery**		**Unseen Gallery**		**Mixed Gallery**	
	mAP_{200}	$Prec_{200}$	mAP_{200}	$Prec_{200}$	mAP_{200}	$Prec_{200}$	mAP_{200}	$Prec_{200}$	mAP_{200}	$Prec_{200}$	mAP_{200}	$Prec_{200}$
ProS*	57.98	54.42	52.19	49.56	76.48	71.86	72.28	68.15	60.52	56.26	55.46	51.95
ZS CLIP	50.08	44.74	43.75	38.91	60.37	51.30	56.08	46.91	44.35	38.40	39.80	33.78
VPT-D	57.70	53.82	50.72	47.29	73.94	68.99	68.81	63.98	57.85	53.42	51.78	47.82
AdaptFormer	57.55	53.59	51.13	47.47	77.24	72.10	72.44	67.56	60.19	55.66	54.47	50.41
IVLP	58.95	55.10	52.11	48.68	73.44	68.38	68.57	63.63	57.44	53.11	51.46	47.61
IVLA	56.62	52.61	50.08	47.39	76.27	72.02	72.44	67.48	59.42	55.47	54.04	50.39
MaPLe	60.65	57.36	53.94	51.08	77.08	72.30	71.99	67.56	60.86	56.68	55.07	51.41
MMA	58.08	56.40	51.46	48.16	77.92	73.43	72.97	68.81	61.02	56.93	55.19	51.61
MAIL	**61.65**	**58.81**	**55.06**	**52.70**	**79.29**	**75.31**	**74.61**	**71.05**	**62.80**	**59.10**	**57.01**	**53.85**

Table 21: 3-shot U^DCDR evaluation results (%) on DomainNet.

Methods	*Sketch*		*Quickdraw*		*Painting*		*Infograph*		*Clipart*		*Average*	
	mAP_{200}	$Prec_{200}$	mAP_{200}	$Prec_{200}$	mAP_{200}	$Prec_{200}$	mAP_{200}	$Prec_{200}$	mAP_{200}	$Prec_{200}$	mAP_{200}	$Prec_{200}$
ProS*	73.85	49.11	28.89	11.86	72.27	46.15	60.56	39.62	81.05	52.98	63.32	39.94
ZS CLIP	47.60	28.71	8.67	4.50	55.69	31.70	47.56	29.36	55.81	31.10	43.07	25.07
VPT-D	68.21	45.24	22.76	10.09	68.17	42.51	60.59	39.10	75.14	47.89	58.61	36.75
AdaptFormer	71.93	46.63	24.77	10.68	69.15	41.88	59.36	38.39	76.87	47.61	60.42	37.03
IVLP	67.46	44.41	22.68	9.66	67.96	42.08	60.15	38.30	74.37	46.90	58.52	36.27
IVLA	72.16	46.62	24.94	10.64	68.88	41.69	59.19	38.13	76.80	47.41	60.39	36.90
MaPLe	71.91	47.27	25.92	10.82	71.41	44.92	61.97	39.85	78.29	49.38	61.90	38.45
MMA	73.44	48.39	26.53	11.27	70.84	43.94	60.43	39.38	78.86	50.33	62.02	38.66
MAIL	**75.65**	**50.54**	**27.30**	**11.24**	**74.18**	**47.23**	**64.37**	**41.91**	**80.99**	**53.45**	**64.50**	**40.87**

Table 22: 3-shot U^CCDR evaluation results (%) on Sketchy and TU-Berlin.

Methods	**Sketchy**		**TU-Berlin**	
	mAP_{200}	$Prec_{200}$	mAP_{all}	$Prec_{100}$
ProS*	69.91	65.45	66.75	74.42
ZS CLIP	35.82	33.08	31.45	46.12
VPT-D	67.03	63.32	63.35	71.52
AdaptFormer	63.97	58.79	65.44	73.22
IVLP	64.72	60.48	60.95	69.54
IVLA	64.36	59.12	64.97	73.02
MaPLe	73.28	69.44	66.72	73.93
MMA	69.74	65.14	67.39	74.12
MAIL	**75.73**	**71.61**	**68.28**	**74.51**

I.3 4-Shot Results

Table 23: 4-shot UCDR evaluation results (%) on DomainNet.

Methods	*Sketch*				*Quickdraw*				*Painting*			
	Unseen Gallery		**Mixed Gallery**		**Unseen Gallery**		**Mixed Gallery**		**Unseen Gallery**		**Mixed Gallery**	
	mAP_{200}	$Prec_{200}$	mAP_{200}	$Prec_{200}$	mAP_{200}	$Prec_{200}$	mAP_{200}	$Prec_{200}$	mAP_{200}	$Prec_{200}$	mAP_{200}	$Prec_{200}$
ProS*	64.67	60.01	58.43	54.63	28.42	25.44	23.18	21.27	75.16	69.55	71.20	66.12
ZS CLIP	42.20	35.28	36.62	29.79	7.44	5.61	6.00	3.17	61.68	55.07	56.53	50.14
VPT-D	62.30	57.65	54.61	50.52	26.01	23.32	19.96	18.27	74.32	68.36	69.21	63.70
AdaptFormer	65.22	61.11	58.58	54.73	28.83	26.07	22.36	20.89	75.11	69.52	70.33	65.18
IVLP	62.06	57.59	54.58	50.72	23.83	21.38	18.19	16.68	73.64	67.91	68.47	63.15
IVLA	65.57	61.04	58.52	54.57	27.24	25.83	21.83	20.81	74.97	69.40	70.09	64.95
MaPLe	65.76	61.43	58.61	54.86	28.46	25.80	22.42	20.72	75.41	69.86	70.76	65.62
MMA	66.65	62.36	59.80	55.99	28.54	26.20	22.70	21.22	75.49	70.04	70.64	65.66
MAIL	**68.74**	**64.64**	**61.93**	**58.39**	**30.24**	**27.82**	**23.77**	**22.37**	**77.37**	**72.20**	**72.46**	**67.80**

Methods	*Infograph*				*Clipart*				*Average*			
	Unseen Gallery		**Mixed Gallery**		**Unseen Gallery**		**Mixed Gallery**		**Unseen Gallery**		**Mixed Gallery**	
	mAP_{200}	$Prec_{200}$	mAP_{200}	$Prec_{200}$	mAP_{200}	$Prec_{200}$	mAP_{200}	$Prec_{200}$	mAP_{200}	$Prec_{200}$	mAP_{200}	$Prec_{200}$
ProS*	57.98	54.42	52.19	49.56	76.48	71.86	72.28	68.15	60.52	56.26	55.46	51.95
ZS CLIP	50.08	44.74	43.75	38.91	60.37	51.30	56.08	46.91	44.35	38.40	39.80	33.78
VPT-D	59.10	55.35	52.14	48.79	75.28	70.46	70.20	65.55	59.40	55.03	53.22	49.37
AdaptFormer	57.14	53.44	50.65	47.31	78.11	73.60	73.21	69.05	60.94	56.74	55.02	51.43
IVLP	59.99	56.25	53.21	49.86	74.77	69.82	69.88	65.12	58.86	54.59	52.87	49.10
IVLA	56.77	54.03	51.20	47.78	77.08	72.35	72.19	68.79	60.33	56.53	54.76	51.38
MaPLe	60.48	57.19	53.79	50.80	77.15	72.74	72.02	67.92	61.45	57.40	55.52	51.98
MMA	59.93	56.59	53.50	50.53	78.27	73.90	73.35	69.34	61.78	57.82	55.60	52.55
MAIL	**62.34**	**59.59**	**55.67**	**53.37**	**79.50**	**75.46**	**74.75**	**71.22**	**63.64**	**59.94**	**57.71**	**54.63**

Table 24: 4-shot U^DCDR evaluation results (%) on DomainNet.

Methods	*Sketch*		*Quickdraw*		*Painting*		*Infograph*		*Clipart*		*Average*	
	mAP_{200}	$Prec_{200}$	mAP_{200}	$Prec_{200}$	mAP_{200}	$Prec_{200}$	mAP_{200}	$Prec_{200}$	mAP_{200}	$Prec_{200}$	mAP_{200}	$Prec_{200}$
ProS*	73.85	49.11	28.89	11.86	72.27	46.15	60.56	39.62	81.05	52.98	63.32	39.94
ZS CLIP	47.60	28.71	8.67	4.50	55.69	31.70	47.56	29.36	55.81	31.10	43.07	25.07
VPT-D	70.43	46.26	25.21	10.91	69.31	43.01	60.98	39.39	76.52	48.51	60.49	37.62
AdaptFormer	73.37	48.15	27.03	11.60	70.91	43.90	59.57	39.05	79.06	50.38	61.99	38.62
IVLP	69.90	45.58	24.20	10.29	68.80	42.40	61.58	39.34	75.19	47.25	59.93	36.97
IVLA	73.25	47.76	26.77	11.22	70.37	43.28	59.78	38.88	78.66	49.65	61.76	38.19
MaPLe	73.59	48.62	28.01	11.54	71.59	45.26	61.88	40.59	79.32	51.00	62.88	39.40
MMA	74.39	48.85	27.14	11.42	71.40	44.54	61.18	39.86	79.31	50.86	62.68	39.11
MAIL	**76.26**	**50.56**	**29.31**	**11.95**	**74.98**	**47.53**	**65.33**	**42.44**	**82.03**	**53.52**	**65.58**	**41.20**

Table 25: 4-shot U^CCDR evaluation results (%) on Sketchy and TU-Berlin.

Methods	**Sketchy**		**TU-Berlin**	
	mAP_{200}	$Prec_{200}$	mAP_{all}	$Prec_{100}$
ProS*	69.91	65.45	66.75	74.42
ZS CLIP	35.82	33.08	31.45	46.12
VPT-D	71.55	67.32	67.16	74.78
AdaptFormer	69.76	65.27	67.64	73.98
IVLP	66.36	62.39	62.83	70.88
IVLA	69.79	65.18	66.89	73.94
MaPLe	73.54	69.60	66.76	73.84
MMA	72.20	68.17	68.22	74.46
MAIL	**75.51**	**71.91**	**68.77**	**74.94**

I.4 8-Shot Results

Table 26: 8-shot UCDR evaluation results (%) on DomainNet.

Methods	*Sketch*				*Quickdraw*				*Painting*			
	UnseenGallery		**MixedGallery**		**UnseenGallery**		**MixedGallery**		**UnseenGallery**		**MixedGallery**	
	mAP_{200}	$Prec_{200}$	mAP_{200}	$Prec_{200}$	mAP_{200}	$Prec_{200}$	mAP_{200}	$Prec_{200}$	mAP_{200}	$Prec_{200}$	mAP_{200}	$Prec_{200}$
ProS*	64.67	60.01	58.43	54.63	28.42	25.44	23.18	21.27	75.16	69.55	71.20	66.12
ZS CLIP	42.20	35.28	36.62	29.79	7.44	5.61	6.00	3.17	61.68	55.07	56.53	50.14
VPT-D	64.28	59.77	56.67	52.80	28.67	26.08	22.06	20.20	75.48	69.76	70.35	64.72
AdaptFormer	65.95	62.09	59.03	55.61	28.11	26.20	21.80	20.52	75.15	69.91	70.55	65.70
IVLP	64.37	59.90	56.90	53.07	27.66	25.13	21.15	19.63	75.10	69.54	69.93	64.82
IVLA	67.13	62.89	60.22	56.53	28.78	26.59	22.72	21.36	75.85	70.43	71.09	66.14
MaPLe	66.37	62.25	59.26	55.77	29.83	27.29	23.35	21.75	75.16	69.48	70.37	65.19
MMA	67.44	63.24	60.67	57.04	29.58	27.29	23.40	21.94	75.78	70.43	71.05	66.16
MAIL	**68.72**	**65.01**	**62.22**	**58.56**	**31.41**	**29.06**	**24.08**	**22.79**	**77.21**	**72.15**	**72.41**	**67.62**

Methods	*Infograph*				*Clipart*				*Average*			
	UnseenGallery		**MixedGallery**		**UnseenGallery**		**MixedGallery**		**UnseenGallery**		**MixedGallery**	
	mAP_{200}	$Prec_{200}$	mAP_{200}	$Prec_{200}$	mAP_{200}	$Prec_{200}$	mAP_{200}	$Prec_{200}$	mAP_{200}	$Prec_{200}$	mAP_{200}	$Prec_{200}$
ProS*	57.98	54.42	52.19	49.56	76.48	71.86	72.28	68.15	60.52	56.26	55.46	51.95
ZS CLIP	50.08	44.74	43.75	38.91	60.37	51.30	56.08	46.91	44.35	38.40	39.80	33.78
VPT-D	60.44	57.05	53.35	50.36	77.08	72.45	71.87	67.50	61.19	57.02	54.86	51.12
AdaptFormer	55.72	52.73	49.17	46.50	77.87	73.83	72.70	69.04	60.56	56.95	54.65	51.47
IVLP	61.20	57.83	54.17	51.22	76.79	72.30	71.85	67.41	61.02	56.94	54.80	51.23
IVLA	58.11	54.87	51.48	48.55	78.62	74.32	73.65	69.73	61.70	57.82	55.83	52.46
MaPLe	60.58	57.46	53.93	51.04	77.61	73.03	72.83	68.60	61.91	57.90	55.95	52.47
MMA	60.29	57.38	53.83	51.44	78.48	74.25	73.49	69.68	62.31	58.54	56.49	53.25
MAIL	**62.22**	**59.44**	**55.10**	**53.10**	**79.22**	**75.31**	**74.78**	**71.01**	**63.75**	**60.19**	**57.72**	**54.62**

Table 27: 8-shot U^DCDR evaluation results (%) on DomainNet.

Methods	*Sketch*		*Quickdraw*		*Painting*		*Infograph*		*Clipart*		*Average*	
	mAP_{200}	$Prec_{200}$	mAP_{200}	$Prec_{200}$	mAP_{200}	$Prec_{200}$	mAP_{200}	$Prec_{200}$	mAP_{200}	$Prec_{200}$	mAP_{200}	$Prec_{200}$
ProS*	73.85	49.11	28.89	11.86	72.27	46.15	60.56	39.62	81.05	52.98	63.32	39.94
ZS CLIP	47.60	28.71	8.67	4.50	55.69	31.70	47.56	29.36	55.81	31.10	43.07	25.07
VPT-D	72.76	48.21	27.66	10.13	71.22	44.72	63.77	41.24	79.12	50.57	62.91	38.97
AdaptFormer	75.19	49.58	28.01	11.79	71.71	44.90	60.62	40.12	80.44	52.42	63.19	39.76
IVLP	72.29	47.71	27.10	11.24	71.10	44.64	63.79	40.89	78.44	50.11	62.54	38.92
IVLA	74.90	49.47	28.05	11.74	71.80	44.88	60.99	40.04	80.23	51.53	63.19	39.53
MaPLe	74.60	49.62	29.54	12.08	71.84	45.27	63.06	40.93	79.45	51.23	63.70	39.75
MMA	75.38	49.97	28.52	11.87	72.26	45.12	62.82	41.14	80.38	51.66	63.87	39.95
MAIL	**76.87**	**51.53**	**30.76**	**12.67**	**75.47**	**48.22**	**65.79**	**42.92**	**81.99**	**53.74**	**66.17**	**41.81**

Table 28: 8-shot U^CCDR evaluation results (%) on Sketchy and TU-Berlin.

Methods	**Sketchy**		**TU-Berlin**	
	mAP_{200}	$Prec_{200}$	mAP_{all}	$Prec_{100}$
ProS*	69.91	65.45	66.75	74.42
ZS CLIP	35.82	33.08	31.45	46.12
VPT-D	70.86	67.19	66.79	74.44
AdaptFormer	74.51	70.98	68.42	73.24
IVLP	70.08	66.24	65.23	72.83
IVLA	74.48	70.70	68.84	74.46
MaPLe	74.86	70.98	67.66	74.27
MMA	75.08	71.63	**68.94**	**74.66**
MAIL	**76.22**	**72.78**	68.91	74.61